consequently leading to the degradation of α-synuclein via a proteasome-dependent proteolytic pathway. Therefore, to measure and quantify the intracellular proteasome-mediated proteolysis, a jellyfish GFP-based reporter was used as a substrate of proteasomal protein degradation (26). As expected, the fluorescence intensity from poly-Ub-GFPs ($Ub^{G76V}GFP$) remarkably decreased in parkin-overexpressed cells. However, the fluorescent level of $Ub^{G76V}GFP$ still decreased in the presence of a specific proteasome inhibitor, clastolactacystin β-lactone, suggesting that parkin may potentiate the degradation of $Ub^{G76V}GFP$, regardless of the inhibition of proteasomal activity. Therefore, we tested the additional possibility that parkin may induce other proteasome-independent protease(s) and attempted to detect this protease.

First, we checked whether cysteine protease caspases are activated by the transient transfection of parkin. Caspase is of particular interest, since it appears to be a common downstream apoptosis effector. PARP is widely used as a typical caspase substrate during apoptotic processes in response to many toxic stimuli. As expected, the stimulation of H19-7 cells with a Ser/Thr protein kinase inhibitor, staurosporine, which is known to activate caspase-3, led to the degradation of intact PARP to the 85-kDa fragment. Interestingly, when the cells were transfected with parkin, an atypical cleavage pattern of PARP was generated. Instead of producing the 85-kDa fragment, parkin caused the formation of the 32-kDa fragment. Tamade *et al.* and Pink *et al.* (27, 37) reported that atypical PARP cleavage is generated by calpains, a family of calcium-requiring intracellular proteases, but not by caspase-3, during β-lapachone-mediated apoptosis. In accordance with the previous findings, degenerated dopaminergic neurons located in the substantia nigra area of PD patients are particularly sensitive to oxidative stresses and are prone to exhibit an elevated internal Ca^{2+} concentration (38). The role of calpain in the degeneration process was suggested after increased expression levels of *m*-calpain were found in the mesencephalon region of a PD patient (39). Furthermore, we and Eberz *et al.* (30, 31) previously reported that α-synuclein could be digested by calpain *in vitro*.

When we determined that parkin might lead to the degradation of α-synuclein via the activation of intracellular calpain *in vivo*, we detected that the production of the smaller PARP fragment was selectively suppressed in the presence of a calpain inhibitors, such as calpeptin and calpastatin peptide. Furthermore, the activity of calpain, but not of caspase, increased in parkin-expressed H19-7 cells, and it was selectively inhibited by calpeptin and calpastatin peptide. The amount of intracellular α-synuclein decreased in parkin-overexpressed cells. Furthermore, the accumulated levels of α-synuclein did not change during the blockade of proteasome activity. Additionally, the parkin-mediated scavenging of the cytotoxic effect of α-synuclein contributes an increase in cell viability in H19-7 cells. The suppression of cell death by parkin was blocked in the presence of calpain inhibitors. These data suggest that the cytoprotective effect of parkin is closely associated with the degradation of α-synuclein via the activation of calpain. In addition to cell death, calpains are the supposed regulators of a variety of other cell processes, including cell proliferation (40), differentiation (41), and transformation (42).

It was recently reported that parkin interacts with the *O*-glycosylated form of α-synuclein but not with its intact form (13). Parkin directly ubiquitinates *O*-glycosylated α-synuclein, which is abundantly accumulated in the brains of parkin-deficient autosomal recessive PD patients, and the loss of parkin function causes pathological accumulation of α-synuclein. The dynamic glycosylation of serine or threonine residues on nuclear and cytoplasmic proteins by *O*-GlcNAc is abundant in all multicellular eukaryotes. The diversity of proteins modified by *O*-GlcNAc implies its importance in many basic cellular and disease processes (43). For example, several proteins that are thought to be involved in Alzheimer's disease, including Tau, AP3, and the β-amyloid precursor protein, are modified by *O*-GlcNAc, and *O*-GlcNAc levels are perturbed in this disease state (25). In contrast, our data show that parkin directly interacts with nonglycosylated α-synuclein in hippocampal H19-7 cells. This discrepancy may result from the fact that H19-7 cells originate from the embryonic stage of rat hippocampus, whereas the specific binding between α-synuclein and parkin depends on the neurodevelopmental stage(s). Alternatively, differences in protein-protein interaction may have been the result of differences in specific cellular environments. Consistent with this view, parkin was reported to bind to α-synuclein, which seemed to be nonglycosylated, considering its molecular size in human neuroblastoma BE-M17 cells under basal as well as under oxidative conditions (18). Double staining of PD brains shows that both parkin and α-synuclein are co-localized in the same pathological structures, such as in LB and axonal spheroid, indicating that the interaction between α-synuclein and parkin somehow contributes to the pathophysiology of PD.

Our current finding that parkin enhances calpain activity suggests that mutations in the parkin gene bring about the impairment of the intracellular degradation process of a number of different proteins, subsequently leading to the formation of cytoplasmic inclusions, such as LBs. Nevertheless, LBs were not actually found in mutant parkin-linked AR-JP patients. This contradiction may be explained by the hypothesis that other compensatory E3 enzymes are involved, and with the suppression of parkin E3 activity, other redundant E3 enzymes could be utilized to degrade α-synuclein, thereby preventing the formation of cytoplasmic inclusions. Otherwise, the formation of intracytoplasmic LBs may not in itself be toxic or necessary to explain the pathological degenerative changes occurring in AR-JP. Recently, it has been hypothesized that the real culprit of neurodegeneration is not the amyloid LB deposits but rather the oligomeric intermediates of amyloidogenic proteins on the way to eventual amyloid formation. It is thought that the amyloid formation is a simple end product of the detoxification process, which is designed to protect the cell from the toxic intermediates. Recent studies support the hypothesis that prefibrillar intermediates (protofibrils), and not mature amyloid fibrils, may be the key toxic species in Alzheimer's disease, PD, and Huntington's disease. *In vitro* studies, with two mutants of α-synuclein associated with inherited PD forms, showed that both mutations cause an acceleration of oligomerization but not fibrillization (44). Consistent with the proposed toxic role of protofibrils in Alzheimer's disease, small oligomers of Aβ potently inhibited hippocampal long term potentiation *in vivo*, whereas fibrillar and monomeric forms had no effect (45). In an independent study, when two proteins, not known to be involved in disease, were incubated under conditions where they formed amyloid fibrils, only the prefibrillar intermediates, and not the mature fibrils, caused cytotoxicity (46). Evidence for the toxic role of the prefibrillar intermediates in Huntington's disease comes from the study that disruption of the microtubule cytoskeleton in cell models for huntingtin aggregation unmasks a glutamine length-dependent toxicity, under conditions where the huntingtin protein exists in a completely nonfibrillar state (47).

It may be possible that parkin regulates the activation of cellular proteases other than calpain, such as granzyme B,

cathepsin, or other exo- and endopeptidases. The effect of parkin on these proteases is currently under investigation. In summary, we demonstrated in this study that parkin accelerates the degradation of α-synuclein via the activation of the nonproteasomal protease, calpain, and that its activation leads to the prevention of the α-synuclein-induced cell death in embryonic hippocampal progenitor cells. A better understanding of parkin's functional significance would greatly contribute to the development of therapeutic modalities for certain forms of PD and to the identification of novel mechanisms for regulating both the protein ubiquitination and protein degradation processes.

Acknowledgments—We are deeply grateful to Drs. B. H. Lee, D. H. Lee, and H. Rhim for helpful discussions, S. W. Jeong and B. H. Jeon for technical assistance with single cell microinjection, and J. Roberts for reading the manuscript. We also thank Dr. M. Masucci (Karolinska Institute, Stockholm, Sweden) for a plasmid encoding jellyfish green fluorescent protein, fused with a noncleavable mutant Ub-moiety, $Ub^{G76V}GFP$.

REFERENCES

1. Lang, A. E., and Lozano, A. M. (1998) *N. Engl. J. Med.* **339,** 1130–1143
2. Golbe, L. I. (1990) *Neurology* **40,** Suppl. 3, 7–14
3. Gasser, T. (2001) *Adv. Neurol.* **86,** 23–32
4. Polymeropoulos, M. H., Lavedan, C., Leroy, E., Ide, S. E., Dehejia, A., Dutra, A., Pike, B., Root, H., Rubenstein, J., Boyer, R., Stenroos, E. S., Chandrasekharappa, S., Athanassiadou, A., Papapetropoulos, T., Johnson, W. G., Lazzarini, A. M., Duvoisin, R. C., Di Iorio, G., Golbe, L. I., and Nussbaum, R. L. (1997) *Science* **276,** 2045–2047
5. Spillantini, M. G., Schmidt, M. L., Lee, V. M., Trojanowski, J. Q., Jakes, R., and Goedert, M. (1997) *Nature* **388,** 839–840
6. Leroy, E., Boyer, R., Auburger, G., Leube, B., Ulm, G., Mezey, E., Harta, G., Brownstein, M. J., Jonnalagada, S., Chernova, T., Dehejia, A., Lavedan, C., Gasser, T., Steinbach, P. J., Wilkinson, K. D., and Polymeropoulos, M. H. (1998) *Nature* **395,** 451–452
7. Kitada, T., Asakawa, S., Hattori, N., Matsumine, H., Yamamura, Y., Minoshima, S., Yokochi, M., Mizuno, Y., and Shimizu, N. (1998) *Nature* **392,** 605–608
8. Saito, M., Maruyama, M., Ikeuchi, K., Kondo, H., Ishukawa, A., Yuasa, T., and Tsuji, S. (2000) *Brain Dev.* **22,** (suppl.) 115–117
9. Shimura, H., Hattori, N., Kubo, S., Mizuno, Y., Asakawa, S., Minoshima, S., Shimizu, N., Iwai, K., Chiba, T., Tanaka, K., and Suzuki, T. (2000) *Nat. Genet.* **25,** 302–305
10. Zhang, Y., Gao, J., Chung, K. K., Huang, H., Dawson, V. L., and Dawson, T. M. (2000) *Proc. Natl. Acad. Sci. U. S. A.* **97,** 13354–13359
11. Hattori, N., Shimura, H., Kubo, S., Kitada, T., Wang, M., Asakawa, S., Minashima, S., Shimizu, N., Suzuki, T., Tanaka, K., and Mizuno, Y. (2000) *Neuropathology* **20,** (suppl.) 85–90
12. Shimura, H., Hattori, N., Kubo, S., Yoshikawa, M., Kitada, T., Matsumine, H., Asakawa, S., Minoshima, S., Yamamura, Y., Shimizu, N., and Mizuno, Y. (1999) *Ann. Neurol.* **45,** 668–672
13. Shimura, H., Schlossmacher, M. G., Hattori, N., Frosch, M. P., Trockenbacher, A., Schneider, R., Mizuno, Y., Kosik, K. S., and Selkoe, D. J. (2001) *Science* **293,** 263–269
14. Solano, S. M., Miller, D. W., Augood, S. J., Young, A. B., and Penney, J. B. (2000) *Ann. Neurol.* **47,** 201–210
15. Peng, X. R., Jia, Z., Zhang, Y., Ware, J., and Trimble, W. S. (2002) *Mol. Cell Biol.* **22,** 378–387
16. Imai, Y., Soda, M., Inoue, H., Hattori, N., Mizuno, Y., and Takahashi, R. (2001) *Cell* **105,** 891–902
17. Schlossmacher, M. G., Frosch, M. P., Gai, W. P., Medina, M., Sharma, N., Forno, L., Ochiishi, T., Shimura, H., Sharon, R., Hattori, N., Langston, J. W., Mizuno, Y., Hyman, B. T., Selkoe, D. J., and Kosik, K. S. (2002) *Am. J. Pathol.* **160,** 1655–1667
18. Choi, P., Golts, N., Snyder, H., Chong, M., Petrucelli, L., Hardy, J., Sparkman, D., Cochran, E., Lee, J. M., and Wolozin, B. (2001) *Neuroreport* **12,** 2839–2843
19. Eves, E. M., Tucker, M. S., Roback, J. D., Downen, M., Rosner, M. R., and Wainer, B. H. (1992) *Proc. Natl. Acad. Sci. U. S. A.* **89,** 4373–4377
20. Chung, K. C., Park, J. H., Kim, C. H., and Ahn, Y. S. (1999) *J. Neurochem.* **72,** 1482–1488
21. D'Agata, V., Zhao, W., and Cavallaro, S. (2000) *Brain Res. Mol. Brain Res.* **75,** 345–349
22. Sung, J. Y., Kim, J., Paik, S. R., Park, J. H., Ahn, Y. S., and Chung, K. C. (2001) *J. Biol. Chem.* **276,** 27441–27448
23. Imai, Y., Soda, M., and Takahashi, R. (2000) *J. Biol. Chem.* **275,** 35661–35664
24. Hsu, L. J., Mallory, M., Xia, Y., Veinbergs, I., Hashimoto, M., Yoshimoto, M., Thal, L. J., Saitoh, T., and Masliah, E. (1998) *J. Neurochem.* **71,** 338–344
25. Comer, F. L., and Hart, G. W. (2000) *J. Biol. Chem.* **275,** 29179–29182
26. Dantuma, N. P., Lindsten, K., Glas, R., Jellne, M., and Masucci, M. G. (2000) *Nat. Biotechol.* **18,** 538–543
27. Tamada, Y., Fukiage, C., Nakamura, Y., Azuma, M., Kim, Y. H., and Shearer, T. R. (2000) *Biochem. Biophys. Res. Commun.* **275,** 300–306
28. Sasaki, T., Kikuchi, T., Yumoto, N., Yoshimura, N., and Murachi, T. (1984) *J. Biol. Chem.* **259,** 12489–12494
29. Rosser, B. G., and Gores, G. J. (2000) *Methods Mol. Biol.* **144,** 245–259
30. Paik, S. R., Lee, J. H., Kim, D. H., Chang, C. S., and Kim, J. (1997) *Arch. Biochem. Biophys.* **344,** 325–334
31. Mishizen-Eberz, A. J., Guttmann, R. P., Giasson, B. I., Day, G. A., Hodara, R., Ischiropoulos, H., Lee, V. M., Trojanowski, J. Q., and Lynch, D. R. (2003) *J. Neurochem.* **86,** 836–847
32. Braak, H., Sandmann-Keil, D., Gai, W., and Braak, E. (1999) *Neurosci. Lett.* **265,** 67–69
33. Munoz, E., Oliva, R., Obach, V., Marti, M. J., Pastor, P., Ballesta, F., and Tolosa, E. (1997) *Neurosci. Lett.* **235,** 57–60
34. Giasson, B. I., and Lee, V. M. (2001) *Neuron* **31,** 885–888
35. Coux, O., Tanaka, K., and Goldberg, A. L. (1996) *Annu. Rev. Biochem.* **65,** 801–847
36. Baumeister, W., Walz, J., Zuhl, F., and Seemuller, E. (1998) *Cell* **92,** 367–380
37. Pink, J. J., Davis, S. W., Tagliarino, C., Planchon, S. M., Yang, X., Froelich, C. J., and Boothman, D. A. (2000) *Exp. Cell Res.* **255,** 144–155
38. Hirsch, E. C., Faucheux, B., Damier, P., Mouatt-Prigent, A., and Agid, Y. (1997) *J. Neural Transm. Suppl.* **50,** 79–88
39. Mouatt-Prigent, A., Karlason, J. O., Agid, Y., and Hirsch, E. C. (1996) *Neuroscience* **73,** 979–987
40. Xu, Y., and Mellgren, R. L. (2002) *J. Biol. Chem.* **277,** 21474–21479
41. Saito, Y., Saido, T. C., Sano, K., and Kawashima, S. (1994) *FEBS Lett.* **353,** 327–331
42. Carragher, N. O., Westhoff, M. A., Riley, D., Potter, D. A., Dutt, P., Elce, J. S., Greer, P. A., and Frame, M. C. (2002) *Mol. Cell Biol.* **22,** 257–269
43. Wells, L., Vossellers, K., and Hart, G. W. (2001) *Science* **291,** 2376–2378
44. Conway, K. A., Lee, S. J., Rochet, J. C., Ding, T. T., Williamson, R. E., and Lansbury, P. T. (2000) *Proc. Natl. Acad. Sci. U. S. A.* **97,** 571–576
45. Walsh, D. M., Klyubin, I., Fadeeva, J. V., Cullen, W. K., Anwyl, R., Wolfe, M. S., Rowan, M. J., and Selkoe, D. J. (2002) *Nature* **416,** 535–539
46. Bucciantini, M., Giannoni, E., Chiti, F., Baroni, F., Formigli, L., Zurdo, J., Taddei, N., Ramponi, G., Dobson, C. M., and Stefani, M. (2002) *Nature* **416,** 507–511
47. Muchowski, P. J., Ning, K., D'Souza-Schorey, C., and Fields, S. (2002) *Proc. Natl. Acad. Sci. U. S. A.* **99,** 727–732
48. Shaw, P., Freeman, J., Bovey, R., and Iggo, R. (1996) *Oncogene* **12,** 921–930

Oncogene (2004) 23, 1645–1655

www.nature.com/onc

ORIGINAL PAPERS

Cbl-c suppresses v-Src-induced transformation through ubiquitin-dependent protein degradation

Minsoo Kim[1], Tohru Tezuka[1], Keiji Tanaka[2] and Tadashi Yamamoto*[,1]

[1]*Division of Oncology, Department of Cancer Biology, The Institute of Medical Science, The University of Tokyo, 4-6-1 Shirokanedai, Minato-ku, Tokyo 108-8639, Japan;* [2]*Department of Molecular Oncology, The Tokyo Metropolitan Institute of Medical Science, 3-18-22 Honkomagome, Bunkyo-ku, Tokyo 113-8613, Japan*

The Cbl family proteins Cbl, Cbl-b, and Cbl-c/Cbl-3 are thought to regulate signaling through protein-tyrosine kinases, positively as scaffold proteins and negatively as ubiquitin ligases. However, the precise signaling pathways and target proteins for each Cbl family member are not well understood. Here we show that Src is a preferential target of Cbl-c for degradation. Although exogenous expression of all Cbl family proteins suppressed the anchorage-independent growth of v-Src-transformed NIH3T3 cells, only Cbl-c caused reversion of the refractile morphology. The level of v-Src protein was reduced by Cbl-c, possibly through a lysosome-dependent pathway. The TKB domain and RING finger of Cbl-c were important for its antioncogenic activity. Wild-type Cbl-c promoted ubiquitination of Src in 293T cells, whereas a RING finger mutant did not. Cbl-c bound specifically to Src phosphorylated at Tyr419. Furthermore, Cbl-c together with UbcH5 induced ubiquitination of Src *in vitro*. Importantly, the Tyr419 nonphosphorylated form of Src was not ubiquitinated by Cbl-c. Therefore, activated Src may be a direct target of Cbl-c *in vivo*. Our results suggest that Cbl and Cbl-b suppress v-Src-induced transformation through mechanisms distinct from that of Cbl-c.
Oncogene (2004) **23**, 1645–1655. doi:10.1038/sj.onc.1207298
Published online 8 December 2003

Keywords: Cbl family; v-Src; transformation; ubiquitination

Introduction

Ubiquitination plays an important role in many basic cellular processes, including cell cycle progression, transcriptional control, protein sorting, and immune response. Ubiquitination is controlled by a multienzyme cascade that involves E1 (ubiquitin-activating enzyme), E2 (ubiquitin-conjugating enzyme), and E3 (ubiquitin-protein ligase) activities. E3 recruits substrates to the ubiquitin machinery and specifies which proteins are targeted for degradation (Weissman, 2001).

The *v-src* oncogene, the transforming gene of Rous sarcoma virus, encodes a constitutively activated form of c-Src. c-Src is a nonreceptor-type protein tyrosine kinase that is important for various mitogenic signalings and has been implicated in a variety of cancers. v-Src activates a number of signaling proteins and leads to transformation (Bjorge *et al.*, 2000). Constitutive activation of signal transducers and activators of transcription 3 (STAT3), phosphatidylinositol 3-kinase (PI3-K)/Akt, and Ras/mitogen-activated protein kinase (MAPK) was observed in v-Src-transformed cells (Odajima *et al.*, 2000).

The *c-cbl* was identified as a cellular homologue of *v-cbl*, a part of the transforming gene of the Cas-NS-1 retrovirus. Introduction of Cas-NS-1 retrovirus induced the formation of pre- and pro-B lymphomas in mice (Langdon *et al.*, 1989). c-Cbl (called Cbl here after) and two other Cbl homologues, Cbl-b and Cbl-c/Cbl-3 (Cbl-c hereafter), have been identified in vertebrates, as have invertebrate orthologues in *Drosophila melanogaster* (D-Cbl) and *Caenorhabditis elegans* (Sli-1). All Cbl family members share a highly conserved tyrosine-kinase binding (TKB) domain and a RING finger. The sequence homology is less extensive in the carboxy-terminal regions of Cbl family proteins (Thien and Langdon, 2001).

The TKB domain of Cbl recognizes activated tyrosine kinases such as epidermal growth factor receptor (EGFR), platelet-derived growth factor receptor (PDGFR), and Syk (Thien and Langdon, 2001). The RING finger domain was recently shown to recruit the E2 ubiquitin-conjugating protein and function as an E3 ubiquitin ligase (Joazeiro *et al.*, 1999). The studies suggest that Cbl recognizes autophosphorylated tyrosine kinases through its TKB domain and degrades them via its E3 activity.

Although Cbl regulates tyrosine kinases negatively by acting as a ubiquitin ligase, Cbl family proteins can also function as adaptor proteins in tyrosine kinase signaling. For example, Cbl promotes integrin-mediated PI3-K activation (Meng and Lowell, 1998). Cbl-b positively regulates PLCγ2 activation by Btk (Yasuda *et al.*, 2002). Thus, it is important to address the roles of Cbl proteins

*Correspondence: T Yamamoto;
E-mail: tyamamot@ims.u-tokyo.ac.jp
Received 20 June 2003; revised 8 September 2003; accepted 14 October 2003

with respect to the signaling pathways in which they are involved.

Cbl-deficient mice show hyperplastic changes in mammary and lymphoid tissues (Murphy *et al.*, 1998). In contrast, Cbl-b-deficient mice are highly susceptible to autoimmune disease, indicating that Cbl and Cbl-b have distinct roles (Bachmaier *et al.*, 2000; Chiang *et al.*, 2000). However, the restricted phenotypes of *cbl-* and *cbl-b*-deficient mice also suggest that there is functional redundancy among Cbl family members. Determining the target proteins of each Cbl protein will be key to understanding the functions of these proteins.

Previously, we reported that expression of Cbl-c is high in colon and small intestine, and this pattern is different from those of Cbl and Cbl-b (Kim *et al.*, 1999). Elevated levels of Src protein and/or kinase activity have been reported in many colon carcinomas (Irby and Yeatman, 2000). Thus, the ligase responsible for Src ubiquitination may be a potential tumor suppressor. In the present study, we examined the roles of Cbl-c, Cbl, and Cbl-b in the regulation of Src.

Materials and methods

Cell culture assay

Human embryonic kidney 293T cells and PlateE cells were maintained in Dulbecco's modified Eagle's medium (DMEM) containing 10% fetal bovine serum. v-Src-transformed NIH3T3 cells and c-SrcY530F stably expressing NIH3T3 cells were maintained in DMEM containing 10% bovine serum. Retroviral expression of Cbl family proteins and colony formation assay were performed as described previously (Suzuki *et al.*, 2002). To determine the growth rate of the cells, 1.5×10^5 cells were plated on 6-mm dishes, and triplicate dishes were harvested at daily intervals for counting the number of the cells.

Antibodies and reagents

Anti-FLAG mAb (M2) was purchased from Sigma. Anti-influenza hemaglutinin (HA) mAb (12CA5) and anti-green fluorescent protein (GFP) were from Roche Molecular Biochemicals. Streptavidin conjugated to horseradish peroxidase (HRP) was from Amersham Biosciences. Anti-phosphotyrosine mAb (RC-20) was from Transduction Laboratories. Anti-Src (327) and anti-α-tubulin mAb were from Oncogene Science. Anti-Cbl-c polyclonal antibody has been previously described (Kim *et al.*, 1999). Antiphospho-Src (pTyr416) and anti-nonphospho-Src (Tyr416) mAb were from Cell Signaling. Synthetic peptides with the following sequences in human c-Src (CLIEDNEpYTARQR and CLIEDNEYTARQR) were supplied by Dr Ohmi (University of Tokyo).

DNA constructions

For the retroviral expression of Cbl family proteins, the full-length human HA-Cbl cDNA (a gift of Dr Longdon), HA-Cbl-b cDNA (a gift of Dr Lipkowitz), and human Cbl-c cDNA were subcloned into the pMX puro expression vector (a gift of Dr Kitamura). Mutation of Gly276 to Glu, Cys351 to Ala, and deletion of Tyr341 designated ΔY341 were introduced into the human Cbl-c cDNA by site-directed mutagenesis. The human Cbl-c sequence encoding amino-acid residues 1–350, designated TKB, was generated by *Bgl*II-mediated deletion. These cDNAs were then cloned into pME18S-FLAG or its derivative, pME18-GST. For production of bacuroviral GST-Src protein, cDNAs for Src and SrcK298M were cloned into the pFastBAC-GST. The E2s cDNAs were subcloned into the pGEX6P-1 vector. pGEX4T-1-UbcH7 is a kind gift of Dr Yokouchi.

Protein analysis

Transient cell transfection, immunoprecipitation, and immunoblotting were performed as described (Tezuka *et al.*, 1999). For the proteasomal and lysosomal inhibitor experiments, cells were incubated with 40 μM MG132 (Peptide Inst.), 10 μM lactacystin (Peptide Inst.), 10 mM methylamine (Sigma), 20 nM bafilomycine (Sigma), or 100 μM chloroquine (Sigma) at 37°C for 4 h before harvest. To detect ubiquitinated Src in 293T cells, His-ubiquitin conjugated Src was purified as described (Rousseau *et al.*, 1999).

In vitro *binding assay*

Purification of GST-Src (WT or K298M) and *in vitro* kinase reaction were performed as described (Nakazawa *et al.*, 2001). 293T cells that express FLAG-Cbl-c WT or mutants were lysed in TNE buffer and the cleared lysates were incubated with *in vitro* phosphorylated GST-Src (1 μg) at 4°C for 4 h. For peptide-inhibition experiments, a synthetic phospho- or non-phosphorylated peptide that was derived from Src was added during incubation.

In vitro *ubiquitination assay*

GST-E2 proteins were expressed in BL21(DE3) and purified by glutathione-sepharose 4B, and the GST was removed with PreScission™ protease (Amersham). As E3 proteins, GST-Cbl family proteins were expressed in 293T cells and purified. GST-Src was purified and the GST was removed. The *in vitro* ubiquitination assay was performed as described (Honda and Yasuda, 1999).

Results

Cbl proteins suppress anchorage-independent growth of v-Src-transformed NIH3T3 cells

We examined the suppression of v-Src-induced transformation by Cbl proteins, with a retrovirus-mediated expression system that permits the low-level expression of the exogenous protein. We constructed retroviruses encoding mock, wild-type Cbl, wild-type Cbl-b, wild-type Cbl-c, a TKB mutant of Cbl-c (Gly276 to Glu, Cbl-c G276E), and a RING finger mutant of Cbl-c (Cys351 to Ala, Cbl-c C351A). We infected v-Src-transformed NIH3T3 cells with retroviruses, selected infected cells with puromycin, and then examined anchorage-independent growth of the cells. As shown in Figure 1, expression of all the three wild-type Cbl family proteins suppressed v-Src-induced transformation. In contrast, anchorage-independent growth of v-Src-transformed cells was only partially inhibited by Cbl-c C351A and was not affected by Cbl-c G276E. Therefore, the TKB domain and RING finger of Cbl-c appear to be important for antioncogenic activity against v-Src.

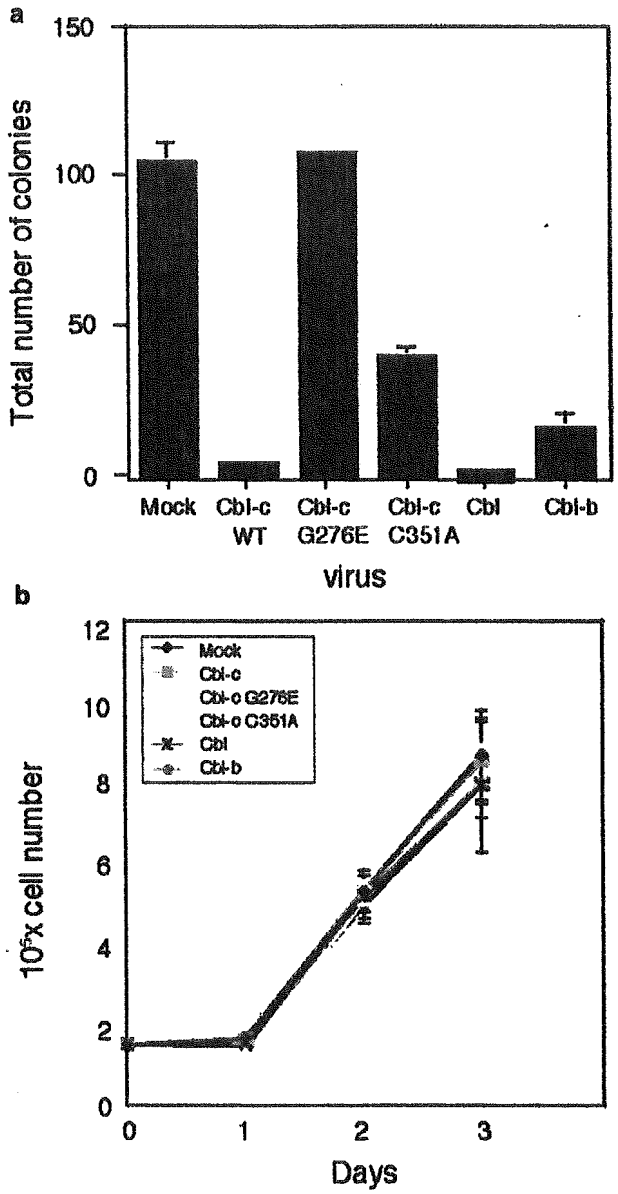

Figure 1 Cbl family proteins suppress anchorage-independent growth of v-Src-transformed NIH3T3 cells. (**a**) v-Src-transformed NIH3T3 cells were infected with the retrovirus carrying mock, Cbl, Cbl-b, or wild-type or mutants of Cbl-c. The infected cells selected by puromycin (1000 cells) were seeded in soft agar. After 2 weeks, the number of drug-resistant colonies was counted. Values are shown as the mean±s.d. of three experiments. (**b**) Growth properties of v-Src-transformed NIH3T3 cells infected with the retroviruses. Infected cells (1.5×10^5) were seeded on 6-mm dishes in triplicate. The number of the cells was counted at daily intervals

Ras-transformed NIH3T3 cells were not affected by retroviruses encoding wild-type Cbl family proteins, indicating that the antioncogenic activities of these viruses are cell-type specific (data not shown). The growth rates of v-Src transformed cells infected with these retroviruses were indistinguishable (Figure 1b).

Cbl-c specifically reduces the levels of v-Src protein and causes reversion of the morphology of v-Src-transformed cells

Another phenotype of transformed cells, refractile morphology, was examined by phase-contrast microscopy. In contrast to the anchorage-independent growth assay, expression of wild-type Cbl-c, but not Cbl, Cbl-b, and Cbl-c mutants, reverted the morphology of v-Src-transformed NIH3T3 cells (Figure 2A). The data suggest that the mechanism of suppression of v-Src-mediated transformation by Cbl-c differs from that by Cbl and Cbl-b.

To address the molecular mechanism by which Cbl-c inhibits v-Src-mediated transformation, we first examined the level of v-Src protein in retrovirus-infected cells. The level of v-Src protein was reduced significantly by expression of wild-type Cbl-c, whereas it was not affected significantly by expression of Cbl, Cbl-b, or Cbl-c mutants (Figure 2B-a). Levels of tyrosine phosphorylation of cellular proteins in v-Src transformed cells were also decreased by expression of wild-type Cbl-c (Figure 2B-e). Retroviral expression of Cbl family proteins was confirmed by immunoblotting (Figure 2B-c and -d). Levels of the p85 subunit of PI3-K and STAT3, downstream effectors of v-Src, were not affected by expression of Cbl family proteins (data not shown). These data, together with the knowledge that Cbl family proteins act as RING-type E3 ubiquitin ligases, suggest that Cbl-c suppresses v-Src-induced transformation through ubiquitination and degradation of v-Src. These findings also indicate that expression of Cbl and Cbl-b suppresses v-Src-mediated transformation through a way distinct from degradation of v-Src.

Degradation of ubiquitinated proteins is mediated by proteasome and lysosomes (Lee *et al.*, 1999). We established an NIH3T3 clone that expresses SrcY530F, an active form of Src. The level of Src in these cells that were infected with the retroviruses was examined in the presence of lysosome inhibitors (methylamine, bafilomycin, and chloroquine) or proteasome inhibitors (MG132 and lactacystin). Cbl-c-mediated degradation of Src was inhibited by lysosome inhibitors but not proteasome inhibitors (Figure 2C, upper panel). Degradation of v-Src by Cbl-c was also inhibited by these lysosome inhibitors (data not shown). These results suggest that Cbl-c degraded v-Src and activated Src through lysosomes.

Cbl-c binds through its TKB domain to Src phosphorylated at Tyr419

A TKB domain mutant, Cbl-c G276E, did not induce degradation of v-Src, suggesting that the phosphorylation-dependent interaction between Cbl-c and Src is critical in degradation of Src. To examine whether Cbl-c interacts with Src directly, 293T cells were transfected with plasmids expressing wild-type Cbl-c, Cbl-c G276E, Cbl-c C351A, Cbl-c TKB, in which the RING finger and a proline-rich region were deleted, and Cbl-c TKB with G276E mutation (Figure 3A). GST-Src fusion protein

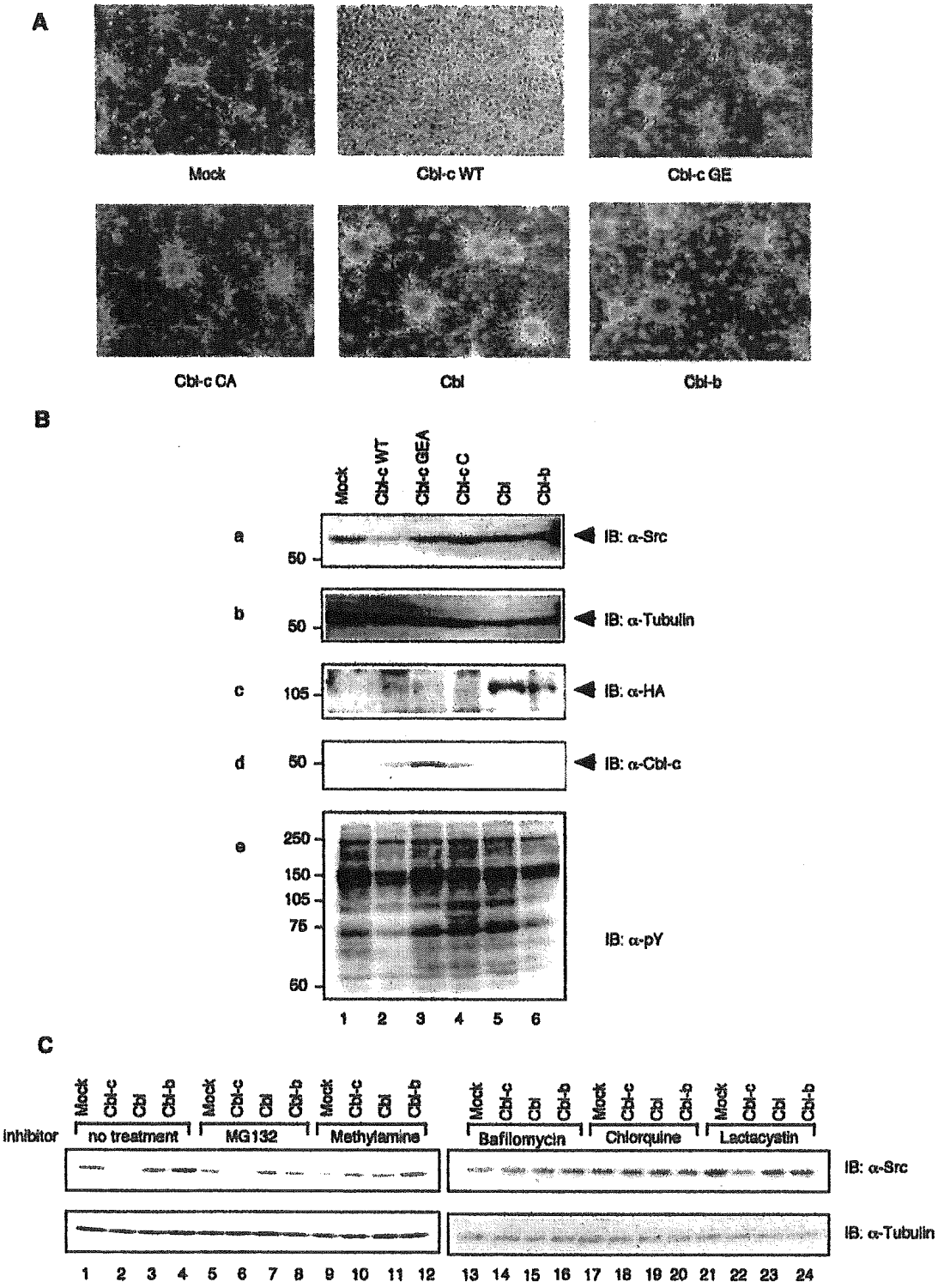

Figure 2 Cbl-c specifically reverts the refractile morphology of v-Src-transformed NIH3T3 cells. v-Src-transformed NIH3T3 cells were infected with the retrovirus as indicated. The infected cells were selected by puromycin. (**A**) Phase-contrast images of the infected cells. (**B**) Lysates of the infected cells were prepared, and analysed by immunoblotting with antibodies against the indicated proteins. (**C**) SrcY530F stable cells were infected with the retrovirus as indicated, and selected by puromycin. The cells were then either untreated (lanes 1–4), or incubated with 40 μM MG132 (lanes 5–8), 10 mM methylamine (lanes 9–12), 20 nM bafilomycine (lanes 13–16), 100 μM chloroquine (lanes 17–20), or 10 μM lactacystin (lanes 21–24) for 4 h. The blots showed the levels of Src and Tubulin as loading controls

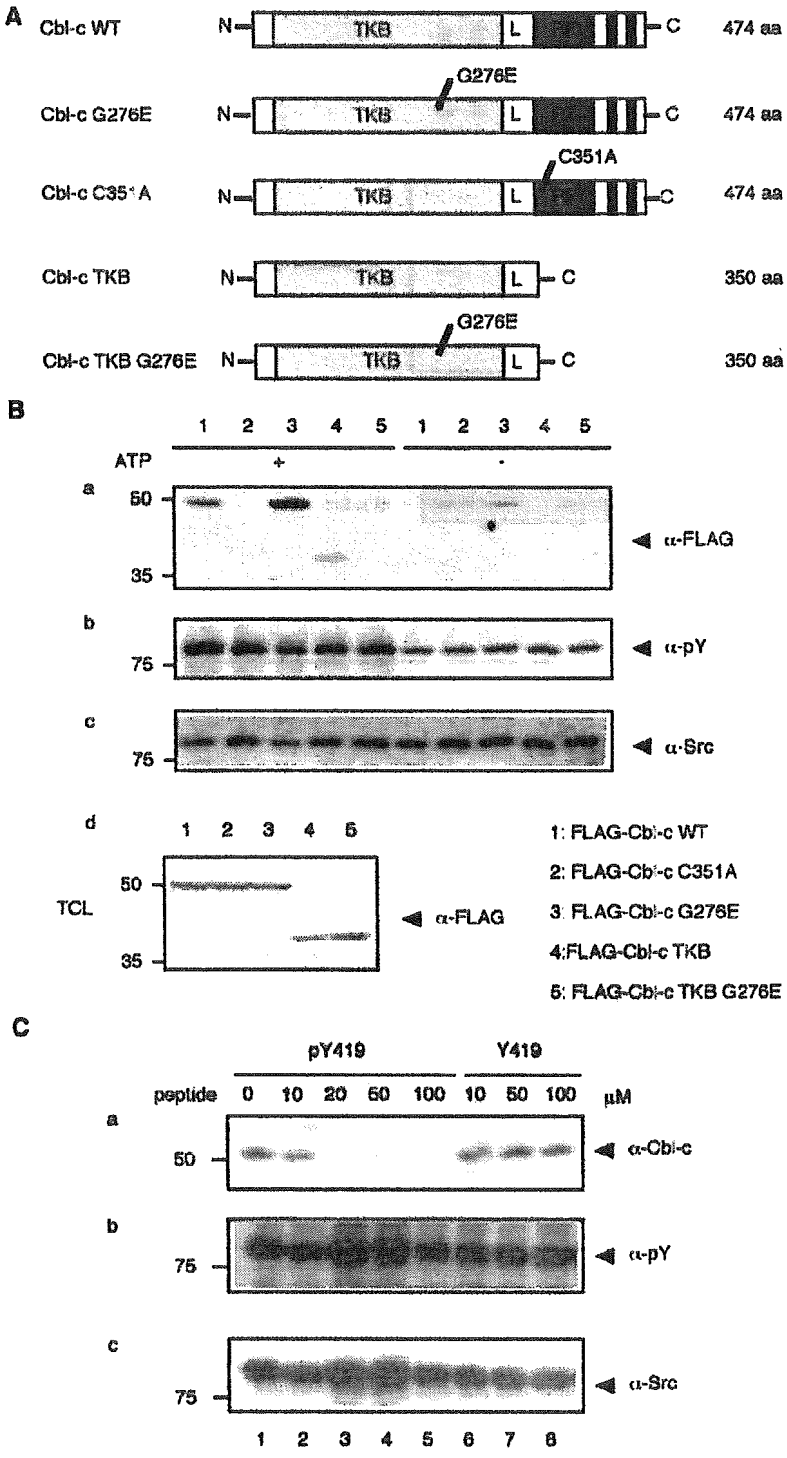

Figure 3 Phosphorylation of Src at Tyr419 is critical for the binding between Cbl-c and Src. (**A**) Schematic diagram of wild-type and mutant Cbl-c. The Gly276 to Glu (G276E) and Cys351 to Ala (C351A) mutations are located in the TKB domain and RING finger, respectively. TKB, tyrosine-kinase binding; RF, RING finger; PRO, proline-rich region. (**B**) GST-Src was immobilized on glutathione-sepharose, and subjected to the kinase reaction in the presence (+) or absence (−) of ATP. Phosphorylated GST-Src was incubated with lysates of 293T cells expressing wild type or mutants of FLAG-Cbl-c. The beads were washed, and then subjected to immunoblotting with anti-FLAG (a). The filter used in (a) was reprobed with anti-pY (b), and anti-Src (c). Levels of FLAG-Cbl-c were confirmed by immunoblotting (d). (**C**) Phosphorylated GST-Src was incubated with lysates of 293T cells expressing wild-type FLAG-Cbl-c in the presence of phosphorylated or nonphosphorylated synthetic peptides corresponding to amino acids 413–424 of Src. pY 419, the Tyr419 phosphorylated peptide; Y419, the Tyr419 nonphosphorylated peptide. The beads were washed, and subjected to immunoblotting with anti-Cbl-c (a). The filter used in (a) was reprobed with anti-pY (b), and anti-Src (c)

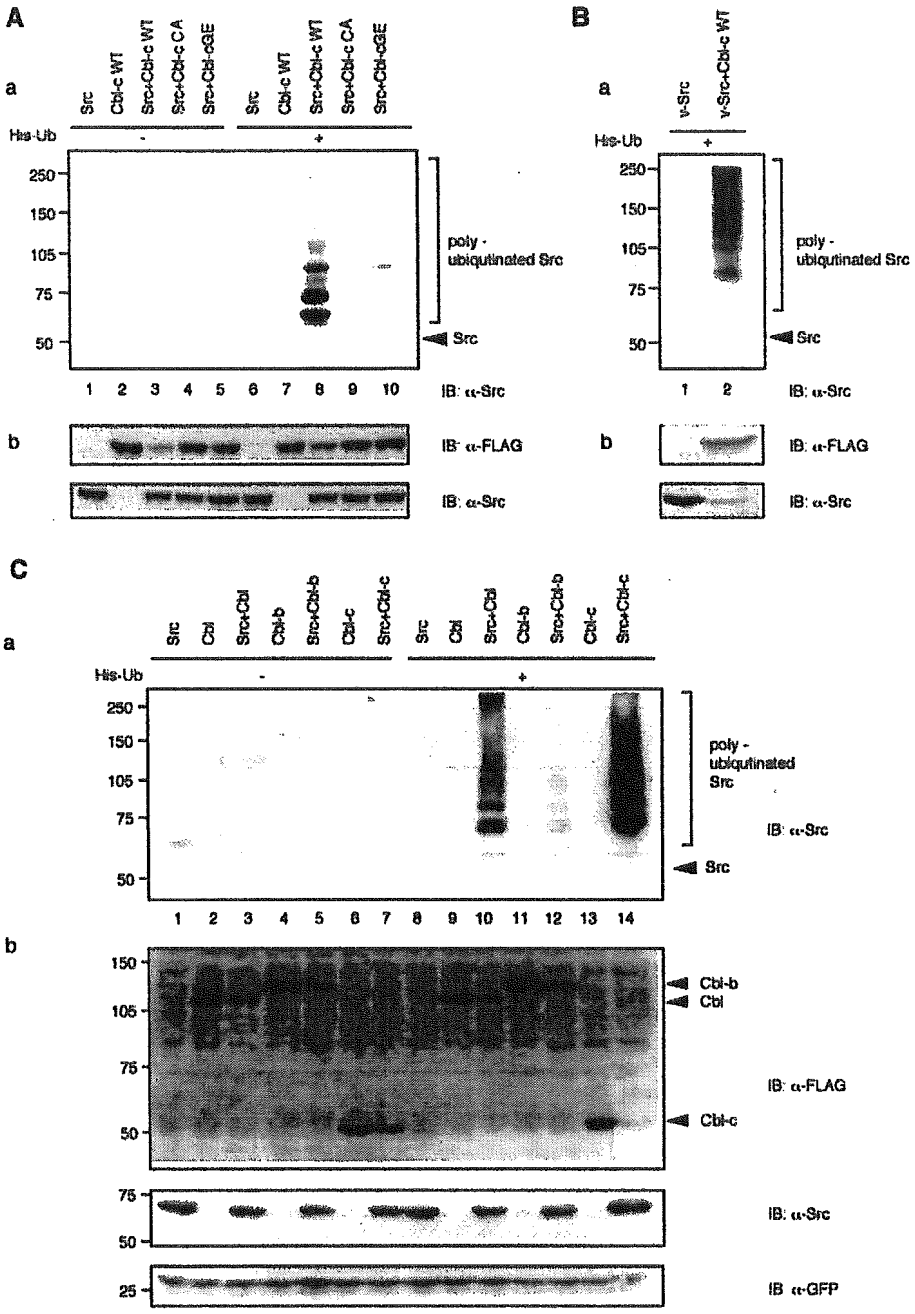

Figure 4 Cbl-c induces ubiquitination of Src in 293T cells. (A) 293T cells were transfected with a combination of the expression plasmids of wild-type and mutants of Cbl-c, c-Src, and His-tagged Ub. The His-Ub conjugated proteins were purified with nickel-NTA agarose, and subjected to immunoblotting with anti-Src. The high molecular weight protein bands representing ubiquitinated forms of Src were observed in the presence of His-Ub, Src and wild-type Cbl-c (lane 8). (B) 293T cells were transfected with expression plasmids of v-Src, wild-type Cbl-c, and His-Ub. (C) 293T cells were transfected with a combination of the expression plasmids of FLAG-Cbl, FLAG-Cbl-b, FLAG-Cbl-c, c-Src, His-Ub, and GFP. Ubiquitinated Src was detected by anti-Src (a). Levels of Cbl-family proteins and Src were confirmed by anti-FLAG and anti-Src (b). Transfection efficiency was confirmed by anti-GFP blotting. Arrowheads indicate the position of Src

was expressed by a baculovirus system, purified, and phosphorylated *in vitro* in the presence or absence of ATP. *In vitro* phosphorylated GST-Src was incubated with lysates of transfected 293T cells, and the amounts of Cbl-c bound to GST-Src were examined (Figure 3B). Wild-type Cbl-c and Cbl-c C351A bound to Src, and this binding was enhanced by phosphorylation of Src. Cbl-c G276E bound slightly to Src, and this binding was independent of Src phosphorylation. Cbl-c TKB bound Src, but this binding was slightly lower than that of wild-type Cbl-c. Furthermore, Cbl-c TKB with G276E mutation did not bind to phosphorylated Src (Figure

3B-a, lane 5). Previously, we reported that Cbl-c interacts with the SH3 domain of Fyn *in vitro* (Kim *et al.*, 1999). These data suggest that Cbl-c binds to phosphorylated Src primarily through the TKB domain. A phosphorylation-independent interaction between the SH3 domain of Src and a proline-rich region of Cbl-c may be involved in the binding of Src and Cbl-c.

Tyr419 and Tyr530 of human Src (Tyr416 and Tyr527 of chicken Src, respectively) are major phosphorylation sites of Src (Bjorge *et al.*, 2000). Tyr419 is highly conserved among Src family members, and the flanking amino-acid sequence confirms to the consensus Cbl docking site (D (D/N) xpYxxxP) (Lupher *et al.*, 1997). To examine if phosphorylation of Src at Tyr419 contributes to binding of Cbl-c with Src, we synthesized tyrosine-phosphorylated and nonphosphorylated peptides that correspond to amino acids 413–424 of Src. As shown in Figure 3C, the phosphopeptide, whereas the nonphosphorylated form did not, inhibited *in vitro* binding between Src and Cbl-c in a dose-dependent manner. These data show that Cbl-c binds to Src, through an interaction between the autophosphorylated Tyr419 of Src and the TKB domain of Cbl-c.

Cbl-c promotes ubiquitination of activated Src in vivo

The level of v-Src was decreased by Cbl-c (Figure 2B), suggesting that Cbl-c acts as a ubiquitin ligase for Src. To study the ubiquitination of Src by Cbl-c, we expressed a combination of wild-type Src, Cbl-c, and histidine epitope-tagged ubiquitin (His-Ub) in 293T cells. Proteins conjugated with His-ubiquitin were purified under denaturing conditions. High molecular weight protein bands for Src, which corresponded to ubiquitinated forms of Src, were observed when wild-type Cbl-c and His-Ub were expressed (Figure 4A-a). v-Src was also ubiquitinated in the presence of Cbl-c (Figure 4B-a). In contrast, a RING finger mutant, Cbl-c C351A, did not promote ubiquitination of Src. These findings indicate that Cbl-c acts as a RING-type ubiquitin ligase for Src *in vivo*. Src was only weakly ubiquitinated by Cbl-c G276E, suggesting that the binding of Cbl-c with Src through its TKB domain is important for ubiquitination of Src (Figure 4A-a).

Moreover, we examined whether Cbl and Cbl-b act as ubiquitin ligases for Src. Coexpression of Cbl and Cbl-b with Src and His-Ub in 293T cells promoted ubiquitination of Src (Figure 4C-a). However, comparison of the level of ubiquitinated Src signal revealed that Cbl-c has the highest ubiquitin ligase activity among Cbl family proteins (Figure 4C-a, lanes 10, 12, and 14). Levels of exogenous proteins were confirmed by immunoblotting (Figure 4A-b, B-b, and C-b). Levels of Cbl-family proteins were decreased by coexpression of Src (see below).

Cbl-c functions as an E3 ubiquitin ligase for Src in vitro

To further understand the mechanism of Src ubiquitination by Cbl-c, we used an *in vitro* ubiquitination assay with recombinant proteins. To date, more than 13 E2 ubiquitin-conjugating enzymes have been identified (Weissman, 2001). To reconstitute the ubiquitination system *in vitro*, we first searched for E2(s) that cooperate with Cbl-c. The *in vitro* ubiquitination reaction was carried out in the presence of E1, ATP, biotinylated Ub, 293T-derived GST-Cbl-c, and E2 proteins. Ubiquitinated proteins were detected with extra-avidin peroxidase. Of nine recombinant E2s tested, self-ubiquitination of Cbl-c was detected in the presence of E2s UbcH4, UbcH5A, UbcH5B, and UbcH5C, indicating that these E2s are coupled functionally with Cbl-c (Figure 5A). Other E2s, including UbcH7, were not active in this assay. We used UbcH5C in our *in vitro* ubiquitination assay. Wild-type (WT) and kinase inactive (K298M) GST-Src were purified, and the GST removed with PreScission™ protease. The *in vitro* ubiquitination assay contained E1, E2 (UbcH5C), E3 (GST-Cbl-c), substrate (WT or K298M Src), ATP, and biotinylated Ub. Each reaction mixture was then subjected to immunoblotting with anti-Src antibody (Figure 5B-a). WT Src, but not K298M Src, was ubiquitinated by Cbl-c *in vitro* (Figure 5B-a, lanes 6 and 7). Similar patterns of high molecular weight protein bands were detected with both anti-Src and extra-avidin peroxidase confirming that these signals corresponded to ubiquitinated Src (Figure 5B-a and -d).

We used phosphorylation state-specific antibodies against Tyr419 of Src, to examine whether ubiquitination of Src requires phosphorylation of Tyr419. As shown in Figures 5B and C, ubiquitinated forms of Src were detected with anti-phospho-Src but not anti-nonphospho-Src, suggesting that Cbl-c specifically promotes ubiquitination of Tyr419 autophosphorylated Src.

Src activates RING-dependent ubiquitin ligase activity of Cbl-c

The structural features of Cbl-c necessary for ubiquitin ligase activity were examined by *in vitro* test of a series of GST-Cbl-c proteins. It was reported that the RING finger and Tyr371 of Cbl were important for E3 ligase activity (Levkowitz *et al.*, 1999; Thien *et al.*, 2001). Ubiquitination of Src by Cbl-c was abolished by the C351A mutation in the RING finger, indicating that the ubiquitin ligase activity of Cbl-c is RING finger dependent *in vitro* (Figure 6A, lane 7). We found that self-ubiquitination of Cbl-c was enhanced in the presence of Src (Figure 6A-c, lanes 5 and 6). It was previously reported that phosphorylation of Cbl at Tyr371 is important for ubiquitin ligase activity (Levkowitz *et al.*, 1999). We constructed a deletion mutant of Cbl-c, Cbl-c ΔY341, in which Tyr341 was deleted. This residue corresponds to Tyr371 of Cbl, and deletion of Tyr371 in Cbl abolishes ubiquitin ligase activity. As expected, Cbl-c ΔY341 showed no ubiquitin ligase activity for Src or itself (Figure 6A, lane 8). However, Src phosphorylated both Cbl-c ΔY341 and wild-type Cbl-c at similar levels, suggesting that Tyr341 of Cbl-c is not phosphorylated at significant levels by Src (Figure 6A-c, lanes 6 and 8).

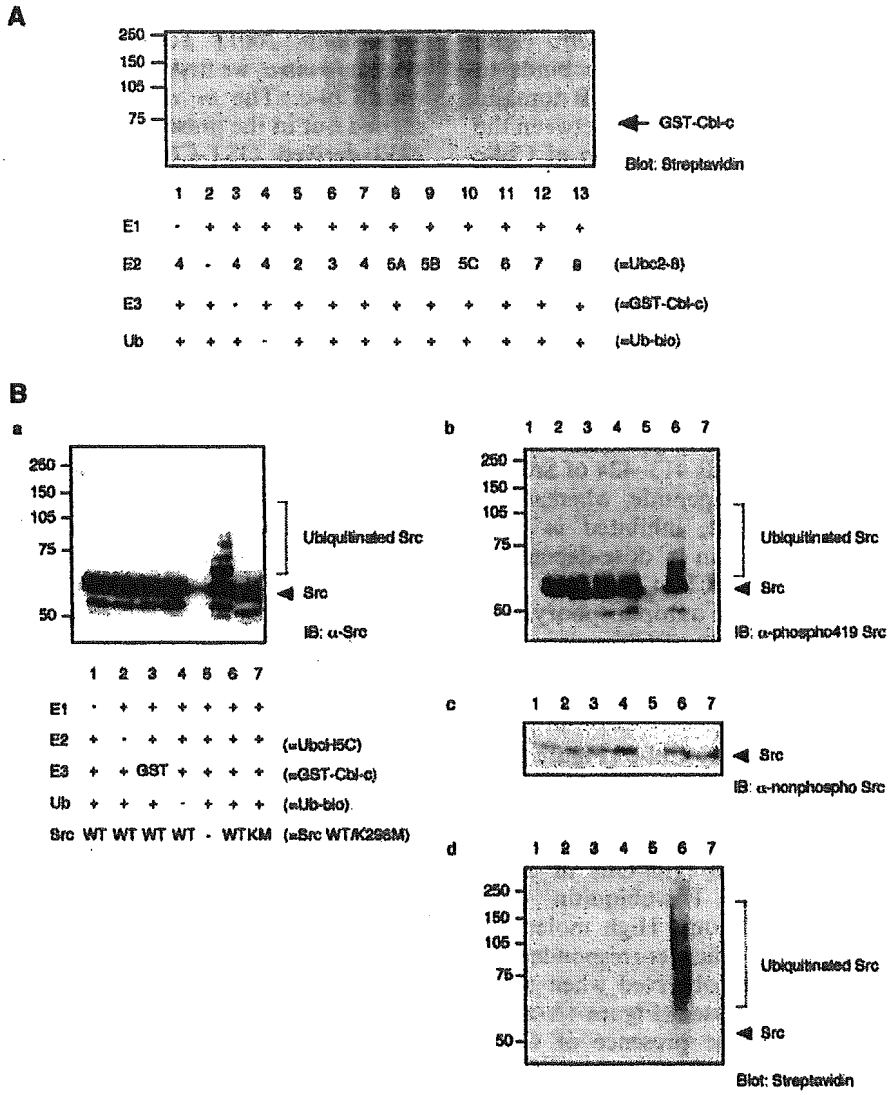

Figure 5 Cbl-c specifically ubiquitinates Src phosphorylated at Tyr419 *in vitro*. (**A**) GST-Cbl-c was incubated with E1, various E2 proteins, and biotinylated ubiquitin. The reaction mixture was subjected to blotting with streptavidin-HRP to detect ubiquitinated proteins. UbcH4, UbcH5A, UbcH5B, and UbcH5C functioned as active E2 for Cbl-c (lanes 7–10). (**B**) Cbl-c ubiquitinates Src *in vitro*. The *in vitro* ubiquitination reaction was performed in the combination of E1, E2 (UbcH5C), GST or GST-Cbl-c as an E3, biotinylated ubiquitin, and wild type or K298M c-Src. GST and GST-Cbl-c were eluted from the glutathione-sepharose. The reaction mixture was probed with anti-Src (a), and streptavidin-HRP (d). The filter used in (a) was reprobed with anti-Tyr419 phosphorylated Src (b), and with anti-Tyr419 nonphosphorylated Src (c). Note that Tyr419 phosphorylated Src, but not nonphosphorylated Src, was specifically ubiquitinated (b and c). Arrowheads indicate the position of Src

Cbl-c contains the strongest ubiquitin ligase activity for Src

Previous studies showed that Cbl promotes ubiquitination of Src when UbcH7 is present as an E2 (Yokouchi *et al*., 2001). However, cooperation of Cbl-c with E2 UbcH7 was absent or much lower in comparison with that with UbcH5C (Figure 5A). To address whether each Cbl protein uses distinct E2s, we compared *in vitro* ubiquitination of Src by Cbl, Cbl-b, and Cbl-c with E2s UbcH5C and GST-UbcH7. Self-ubiquitination of all Cbl family proteins was prominent in the presence of UbcH5C (Figure 6B-a, lanes 6, 8, and 10), confirming that UbcH5C is a functional E2 for all Cbl proteins. In contrast, UbcH7 was not active in our system (Figure 6B-a, lanes 7, 9, and 11). Moreover, Src was ubiquitinated only in the presence of UbcH5C (Figure 6B-b). UbcH7 was also inactive in Cbl- and Cbl-b-induced ubiquitination of Src. Consistent with our results, it has been reported that Cbl ubiquitinates EGFR in cooperation with UbcH5B and UbcH5C, but not UbcH7 *in vitro* (Levkowitz *et al*., 1999).

Among Cbl family proteins, Cbl-c showed the strongest ubiquitin ligase activity for Src *in vitro* (Figure 6B-b, lanes 6, 8, and 10), which is consistent with our results in 293T cells (Figure 4C). Levels of self-ubiquitination and tyrosine phosphorylation were comparable between the different proteins (Figure 6B-a

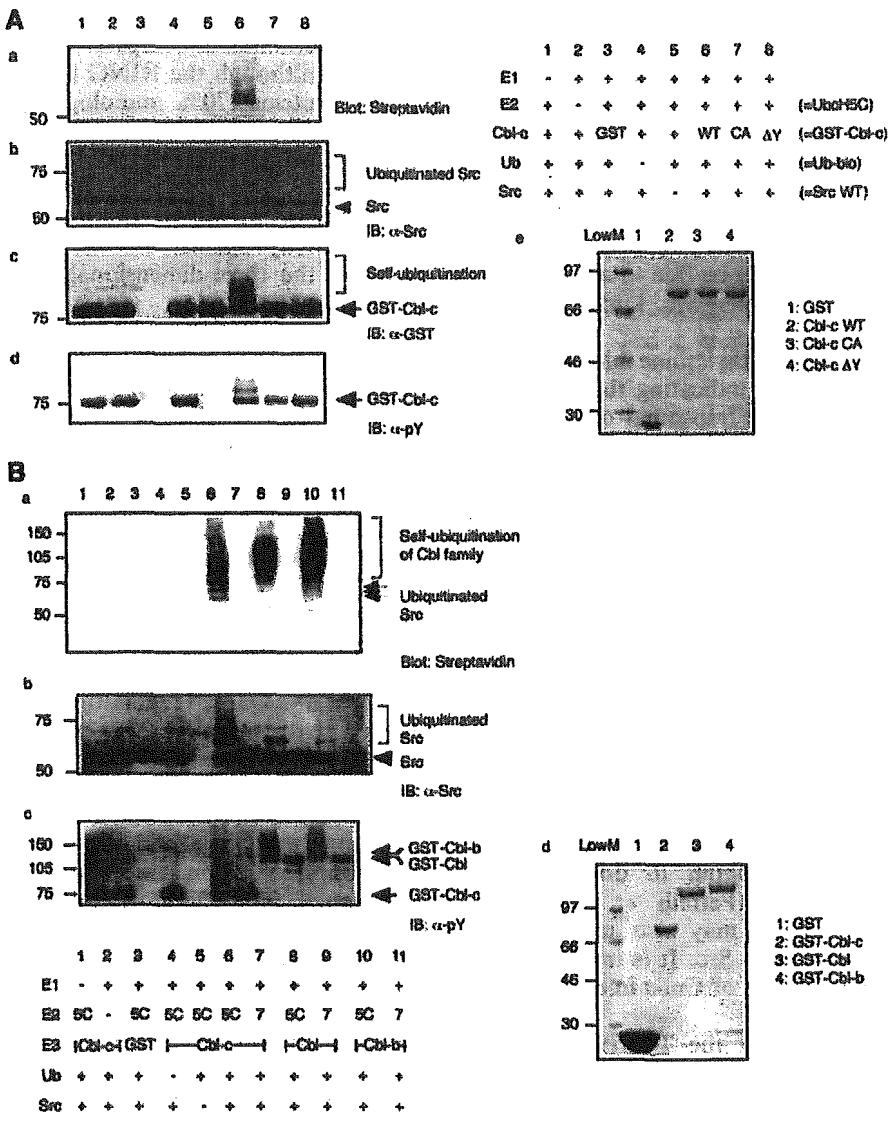

Figure 6 Src activates the ubiquitin ligase activity of Cbl proteins *in vitro*. (**A**) The ubiquitination reaction was performed *in vitro* in the combination of E1, E2 (UbcH5C), E3 (GST, wild type or mutants of GST-Cbl-c), biotinylated ubiquitin, and wild-type c-Src. The mixture was probed with streptavidin-HRP (a). The filter was reprobed with anti-Src (b), anti-GST (c), and anti-pY (d), respectively. (**B**) The ubiquitination of Src was performed using UbcH5C or GST-UbcH7 as an E2, and GST, GST-Cbl, GST-Cbl-b, or GST-Cbl-c as an E3. Ubiquitinated Src was visualized by streptavidin-HRP (a) and anti-Src (b). Arrowheads indicate the position of Src. Arrows indicate the position of GST-Cbl families. The filter used in (a) was reprobed with anti-pY (c). The sizes and purities of the fusion proteins were confirmed by Coomassie brilliant blue R-250 staining (A-e and B-d)

and -c). Self-ubiquitination of Cbl-family proteins was enhanced by Src (Figure 6B-b), suggesting that Cbl-family proteins are also degraded in the presence of active Src (Yokouchi *et al*., 2001). Consistent with these results, the levels of Cbl-family proteins were decreased by coexpression of Src (Figure 4C-b).

Discussion

Here we show that the Cbl-c suppresses v-Src-mediated transformation by degrading v-Src. Cbl-c promotes ubiquitination of activated Src *in vivo*. Moreover, Cbl-c specifically binds to and ubiquitinates Tyr419-phosphorylated Src *in vitro*. Our findings suggest that endogenous Cbl-c is a negative regulator of Src.

Mutation of the TKB domain of Cbl-c (G298E) completely abolishes the antioncogenic activity against v-Src, whereas mutation of the RING finger (C351A) partially suppresses the antioncogenic activity, suggesting the importance of both domains. Cbl inhibits several tyrosine kinases, including EGFR, PDGFR, and Syk (Thien and Langdon, 2001). The TKB domain of Cbl mediates binding to these kinases. We observed that the

TKB domain of Cbl-c binds to Src phosphorylated at Tyr419, which is located in the activation loop of the kinase domain. All Src family kinases, except Blk, have the Cbl TKB-binding motif at the autophosphorylation site, suggesting that Cbl-c also suppresses the activity of these kinases. v-Cbl, which has only a TKB domain, binds to activated Src and inhibits the kinase activity (Sanjay *et al.*, 2001). Since Cbl-c C351A also binds Src, the observed partial inhibition of v-Src-mediated transformation by Cbl-c C351A may be due to a conformational interference that inhibits Src kinase activity toward substrates.

The lysosomal inhibitor methylamine blocks Cbl-c-induced degradation of v-Src, indicating that ubiquitination of Src is relevant to its lysosomal degradation. Cbl-mediated ubiquitination of receptor tyrosine kinases serves as a sorting signal for transport to lysosomes (Levkowitz *et al.*, 1998). Cbl-deficient mice are defective in endocytosis and degradation of pre-T-cell receptor (Panigada *et al.*, 2002). Degradation of nonreceptor-type tyrosine kinases, such as Hck and Syk, is mediated in part by lysosomes (Paolini *et al.*, 2001; Howlett and Robbins, 2002). Some population of Src is associated with endosomal membranes and vesicles in 3T3 fibroblasts and PC12 cells (Kaplan *et al.*, 1992). Another Src-family kinase, Hck, is present in lysosomal vesicles in human macrophages (Astarie-Dequeker *et al.*, 2002). Although the mechanism of protein trafficking to endosomes by Cbl family members is poorly understood, Cbl forms a complex with CIN85-endophilin to downregulate c-Met and EGF receptors (Petrelli *et al.*, 2002; Soubeyran *et al.*, 2002). Cbl-c may also act cooperatively with CIN85 to degrade v-Src. It is important to identify adaptors and activators of Cbl-c in endosomal/lysosomal vesicles.

In this study, we show that the Tyr419 autophosphorylated form of Src is specifically ubiquitinated by Cbl-c. Moreover, Src enhances the ligase activity of Cbl-c against Src and itself. Therefore, Src activation and Cbl-c-induced ubiquitination of Src are strongly correlated. Phosphorylation is a key component of some ubiquitination pathways (Weissman, 2001). The mechanism by which Src enhances the ligase activity of Cbl-c must be analysed further to clarify the activity-dependent regulation of Src by Cbl-c.

We showed that Cbl-c has stronger ubiquitin ligase activity against Src than Cbl and Cbl-b both *in vitro* and *in vivo*, although all Cbl family proteins induce ubiquitination of Src. This difference may explain our observation that expression of Cbl-c, but not Cbl or Cbl-b, significantly downregulates v-Src, and suppresses the anchorage-independent growth of v-Src-transformed cells. Cbl is reported to ubiquitinate Src, and chicken Src with mutation at Tyr416 to Phe (corresponding to human Src Y419F) is weakly ubiquitinated by Cbl (Yokouchi *et al.*, 2001). In addition, Src ubiquitination by Cbl requires the RING finger and proline-rich domains, but not the TKB domain of Cbl. Therefore, the mechanism of Src ubiquitination by Cbl-c is different from that by Cbl. Cbl-c is truncated at the carboxy-terminus in comparison with Cbl and Cbl-b. In addition, although the RING finger is conserved in Cbl family proteins (70% homology), the TKB domain of Cbl-c has less homology than those of Cbl and Cbl-b (48 and 46%, respectively). In contrast, the TKB domains of Cbl and Cbl-b have 84% homology. These distinct structural properties of Cbl-c might explain its higher ligase activity against Src. It would be important to compare the three-dimensional structure of Cbl-family proteins.

Expression of Cbl and Cbl-b suppresses the anchorage-independent growth of v-Src-transformed cells, although they cause no significant decrease in the level of v-Src. These results suggest that Cbl and Cbl-b inhibit the signaling molecules downstream of v-Src. We previously identified an adaptor protein, BLNK, as a target of Cbl in B cells (Yasuda *et al.*, 2002). Cbl-b inhibits signaling mediated by Vav and PI3-K (Krawczyk *et al.*, 2000). Identification of critical target proteins for Cbl and Cbl-b in v-Src-transformed cells would clarify the precise roles of Cbl family proteins in tyrosine kinase signaling.

Our present results strongly suggest that endogenous Cbl-c is a negative regulator of Src. Previously, we showed that *cbl-c* mRNA is expressed at high levels in the colon (Kim *et al.*, 1999). Deregulated Src kinase activity has been implicated in the progression of colon cancer. Src protein levels are increased modestly in adenomatous polyps and increased further during the progression of colon cancer and metastasis (Irby and Yeatman, 2000). Therefore, inhibition of Src by Cbl-c could contribute to tumor suppression in these tissues. Abrogation of Cbl-c could result in cancer progression by activating Src, although chromosomal rearrangements or mutations of the *CBL-C* locus have not been identified. It will be important to establish the role of endogenous Cbl-c in the regulation of tyrosine kinases, including Src, during normal development and in cancer pathology.

Abbreviations

SH 2/3, Src homology 2/3; EGFR, epidermal growth factor receptor; PDGER, platelet-derived growth factor receptor; PI3-K, phosphatidylinositol 3-kinase; STAT3, signal transducers and activators of transcription 3; PY, phosphotyrosine.

Acknowledgements

We thank Y Yoshida and T Yasuda for valuable discussion and technical advice. We thank W Langdon (University of Western Australia), S Lipkowitz (NCI), and M Yokouchi (University of Kagoshima) for cDNAs, T Kitamura (University of Tokyo) for the retrovirus system, and K Iwai (Osaka City University) for mouse E1. We thank T Suzuki and T Chiba (Tokyo Metro. Inst. of Med. Sci.) for critical discussion. This work was supported by grants-in-aid from the Ministry of Education, Culture, Sports, Science, and Technology of Japan. MK is a recipient of the Japanese government scholarship.

References

Astarie-Dequeker C, Carreno S, Cougoule C and Maridonneau-Parini I. (2002). *J. Cell Sci.*, **115**, 81–89.

Bachmaier K, Krawczyk C, Kozieradzki I, Kong YY, Sasaki T, Oliveira-dos-Santos A, Mariathasan S, Bouchard D, Wakeham A, Itie A, Le J, Ohashi PS, Sarosi I, Nishina H, Lipkowitz S and Penninger JM. (2000). *Nature*, **403**, 211–216.

Bjorge JD, Jakymiw A and Fujita DJ. (2000). *Oncogene*, **19**, 5620–5635.

Chiang YJ, Kole HK, Brown K, Naramura M, Fukuhara S, Hu RJ, Jang IK, Gutkind JS, Shevach E and Gu H. (2000). *Nature*, **403**, 216–220.

Honda R and Yasuda H. (1999). *EMBO J.*, **18**, 22–27.

Howlett CJ and Robbins SM. (2002). *Oncogene*, **21**, 1707–1716.

Irby RB and Yeatman TJ. (2000). *Oncogene*, **19**, 5636–5642.

Joazeiro CA, Wing SS, Huang H, Leverson JD, Hunter T and Liu YC. (1999). *Science*, **286**, 309–312.

Kaplan KB, Swedlow JR, Varmus HE and Morgan DO. (1992). *J. Cell Biol.*, **118**, 321–333.

Kim M, Tezuka T, Suziki Y, Sugano S, Hirai M and Yamamoto T. (1999). *Gene*, **239**, 145–154.

Krawczyk C, Bachmaier K, Sasaki T, Jones GR, Snapper BS, Bouchard D, Kozieradzki I, Ohashi SP, Alt WF and Penninger MJ. (2000). *Immunity*, **13**, 463–473.

Langdon WY, Hartley JW, Klinken SP, Ruscetti SK and Morse Hd. (1989). *Proc. Natl. Acad. Sci. USA*, **86**, 1168–1172.

Lee PS, Wang Y, Dominguez MG, Yeung YG, Murphy MA, Bowtell DD and Stanley ER. (1999). *EMBO J.*, **18**, 3616–3628.

Levkowitz G, Waterman H, Ettenberg SA, Katz M, Tsygankov AY, Alroy I, Lavi S, Iwai K, Reiss Y, Ciechanover A, Lipkowitz S and Yarden Y. (1999). *Mol. Cell*, **4**, 1029–1040.

Levkowitz G, Waterman H, Zamir E, Kam Z, Oved S, Langdon WY, Beguinot L, Geiger B and Yarden Y. (1998). *Genes Dev.*, **12**, 3663–3674.

Lupher MJ, Songyang Z, Shoelson SE, Cantley LC and Band H. (1997). *J. Biol. Chem.*, **272**, 33140–33144.

Meng F and Lowell CA. (1998). *EMBO J.*, **17**, 4391–4403.

Murphy MA, Schnall RG, Venter DJ, Barnett L, Bertoncello I, Thien CB, Langdon WY and Bowtell DD. (1998). *Mol. Cell. Biol.*, **18**, 4872–4882.

Nakazawa T, Komai S, Tezuka T, Hisatsune C, Umemori H, Semba K, Mishina M, Manabe T and Yamamoto T. (2001). *J. Biol. Chem.*, **276**, 693–699.

Odajima J, Matsumura II, Sonoyama J, Daino H, Kawasaki A, Tanaka H, Inohara N, Kitamura T, Downward J, Nakajima K, Hirano T and Kanakura Y. (2000). *J. Biol. Chem.*, **11**, 11.

Panigada M, Porcellini S, Barbier E, Hoeflinger S, Cazenave PA, Gu H, Band H, von Boehmer H and Grassi F. (2002). *J. Exp. Med.*, **195**, 1585–1597.

Paolini R, Molfetta R, Piccoli M, Frati L and Santoni A. (2001). *Proc. Natl. Acad. Sci. USA*, **98**, 9611–9616.

Petrelli A, Gilestro GF, Lanzardo S, Comoglio PM, Migone N and Giordano S. (2002). *Nature*, **416**, 187–190.

Rousseau D, Cannella D, Boulaire J, Fitzgerald P, Fotedar A and Fotedar R. (1999). *Oncogene*, **18**, 4313–4325.

Sanjay A, Houghton A, Neff L, DiDomenico E, Bardelay C, Antoine E, Levy J, Gailit J, Bowtell D, Horne WC and Baron R. (2001). *J. Cell. Biol.*, **152**, 181–195.

Soubeyran P, Kowanetz K, Szymkiewicz I, Langdon WY and Dikic I. (2002). *Nature*, **416**, 183–187.

Suzuki T, K-Tsuzuku J, Ajima R, Nakamura T, Yoshida Y and Yamamoto T. (2002). *Genes Dev.*, **16**, 1356–1370.

Tezuka T, Umemori H, Akiyama T, Nakanishi S and Yamamoto T. (1999). *Proc. Natl. Acad. Sci. USA*, **96**, 435–440.

Thien CB and Langdon WY. (2001). *Nat. Rev. Mol. Cell Biol.*, **2**, 294–307.

Thien CB, Walker F and Langdon WY. (2001). *Mol. Cell*, **7**, 355–365.

Weissman AM. (2001). *Nat. Rev. Mol. Cell Biol.*, **2**, 169–178.

Yasuda T, Tezuka T, Maeda A, Inazu T, Yamanashi Y, Gu H, Kurosaki T and Yamamoto T. (2002). *J. Exp. Med.*, **196**, 51–63.

Yokouchi M, Kondo T, Sanjay A, Houghton A, Yoshimura A, Komiya S, Zhang H and Baron R. (2001). *J. Biol. Chem.*, **276**, 35185–35193.

Journal of Neurochemistry, 2003, **86**, 749–762 doi:10.1046/j.1471-4159.2003.01875.x

A palmitoylated RING finger ubiquitin ligase and its homologue in the brain membranes

Kazuaki Araki,*[,1] Meiko Kawamura,*[,1] Toshiaki Suzuki,† Noriyuki Matsuda,† Daiji Kanbe,* Kyoko Ishii,* Tomio Ichikawa,‡ Toshiro Kumanishi,‡ Tomoki Chiba,† Keiji Tanaka† and Hiroyuki Nawa*

**Department of Molecular Neurobiology, Brain Research Institute, Niigata University, Niigata, Japan*

†Molecular Oncology, Tokyo Metropolitan Institute of Medical Science, Bunkyo-ku, Tokyo, Japan

‡Department of Molecular Pathology, Brain Research Institute, Niigata University, Niigata, Japan

Abstract

Ubiquitin (Ub) ligation is implicated in active protein metabolism and subcellular trafficking and its impairment is involved in various neurologic diseases. In rat brain, we identified two novel Ub ligases, Momo and Sakura, carrying double zinc finger motif and RING finger domain. Momo expression is enriched in the brain gray matter and testis, and Sakura expression is more widely detected in the brain white matter as well as in many peripheral organs. Both proteins associate with the cell membranes of neuronal and/or glial cells. We examined their Ub ligase activity *in vivo* and *in vitro* using viral expression vectors carrying myc-tagged Momo and Sakura. Overexpression of either Momo or Sakura in mixed cortical cultures increased total polyubiquitination levels. *In vitro* ubiquitination assay revealed that the combination of Momo and UbcH4 and H5c, or of Sakura and UbcH4, H5c and H6 is required for the reaction. Deletion mutagenesis suggested that the E3 Ub ligase activity of Momo and Sakura depended on their C-terminal domains containing RING finger structure, while their N-terminal domains influenced their membrane association. In agreement, Sakura associating with the membrane was specifically palmitoylated. Although the molecular targets of their Ub ligation remain to be identified, these findings imply a novel function of the palmitoylated E3 Ub ligase(s).

Keywords: glia, membrane protein, neuron, palmitoylation, ubiquitination.

J. Neurochem. (2003) **86**, 749–762.

The RING finger structure, named after a peculiar amino acid sequence found in 'Really Interesting New Gene', represents the zinc binding motif of Cys-X2-Cys-X9/39-Cys-X1/3-His-X2/3-Cys/His-X2-Cys-X4-48-Cys-X2-Cys (Lovering *et al.* 1993). At present, more than 100 members of this family contain this structure and most of them are suggested to function as a ubiquitin (Ub) ligase (E3) (Lorick *et al.* 1999). The RING finger proteins such as APC11 and Rbx1/ROC1 were initially isolated as oncogenes and probed to be E3 enzymes in the APC/C and SCF complexes (Tyers and Willems 1999). Although morphologic neuropathology indicates that brain neurons or glia contain Ub-containing inclusion bodies in a variety of neurologic diseases, biological implication of Ub accumulation in these diseases remains to be characterized (DiFiglia *et al.* 1997; Alves-Rodrigues *et al.* 1998; Hardy and Gwinn-Hardy 1998; Cummings *et al.* 1999). Recent progresses in molecular neurology have revealed that some neurodegenerative diseases involve impaired protein ubiquitination and abnormal proteolysis leading to neuronal death. Parkin, identified as a gene product responsible for familial Parkinsonism, contains RING finger domain and functions as an E3 Ub ligase in the nervous system (Kitada *et al.* 1998; Shimura *et al.* 2000;

Received February 5, 2003; revised manuscript received April 16, 2003; accepted April 30, 2003.

Address correspondence and reprint requests to Hiroyuki Nawa, Division of Molecular Neurobiology, Brain Research Institute, Niigata University, Asahimachi-dori 1–757, Niigata 951–8585, Japan.
E-mail: hnawa@bri.niigata-u.ac.jp

[1]Both authors equally contributed to this work.

Abbreviations used: DTT: dithiothreitol; E1, ubiquitin-activating enzyme; E2, ubiquitin-conjugating enzyme; E3, ubiquitin ligase; IAP, inhibitor of apoptosis; MOI, multiplicity of infection; ORF, open reading frame; PAGE, polyacrylamide gel electrophoresis; PBS, phosphate-buffered saline; PCR, polymerase chain reaction; SDS, sodium dodecyl sulfate; SSC, sodium chloride/sodium citrate buffer; Ub, ubiquitin.

Chung *et al.* 2001b). These observations suggest that the Ub ligase activity of RING finger proteins may contribute to the pathogenesis of many neurodegenerative diseases.

The molecular roles of protein ubiquitination underlying oncogenesis have been intensively investigated and are correlated with catabolism of the regulatory proteins of cell growth and/or the cell cycle (Kamura *et al.* 1999; Joazeiro *et al.* 1999; Skowyra *et al.* 1999; Zachariae and Nasmyth 1999; Honda and Yasuda 2000; Ruffner *et al.* 2001). Although there are many unique membrane proteins in the nervous system, only a few E3 ligases corresponding to the substrates have been identified (i.e. Parkin, Siah and NEDD4). Siah is an enzyme that transfers Ub to the netrin-1 receptor, DDC (deleted in colorectal cancer), and is suggested to control degradation of the metabotropic glutamate receptor 1 (Hu and Fearon 1999; Ishikawa *et al.* 1999). NEDD4 is another member of the Ub ligase family that shares a common protein motif named HECT (homologous to E6AP C-terminus) and ubiquitinates amiloride-sensitive sodium channels (Staub *et al.* 1997). Although most of the targets for Ub ligases localize at special subcellular membrane components to exert their unique functions, the interaction of the Ub ligase with membranes is often indirect and mediated by other molecules (Kavsak *et al.* 2000; Shenoy *et al.* 2001; Soubeyran *et al.* 2002). Thus, it remains to be determined how membrane-bound neural proteins are ubiquitinated and catabolized in neurons and glia, and whether the dysfunction of these processes is associated with human neurodegenerative diseases.

In the present study, we have characterized the novel E3 Ub ligase and its homologue that both associate with neural cell membranes. Their distributions in the brain as well as their enzyme activities as a Ub ligase are examined and discussed.

Materials and methods

cDNA library screening

A Sal I-EcoR I genomic fragment spanning 75 bp (849–923 nt; AATCCTGGCTCGGAATTTTGTCAACTATTCTGGCTGCTGTGAAAAGTGGGAGCTGGTGGAGAAAGTCAACCGGCT) was isolated as a part of the down-stream gene by monitoring the binding activity of the neuronal transcription factor HIT-4 (Hirano *et al.* 2001). Subsequently, 300 000 plaques of the lambda Zap library carrying rat hippocampal cDNA (Stratagene, La Jolla, CA, USA) were screened against the genomic sequence. Eleven clones were isolated and subjected to automatic DNA sequencing (ABI 7700; Applied Bio Instruments, Foster City, CA, USA). All positive clones contained the same sequence and one clone contained a 1952-bp cDNA corresponding to a full open reading frame of Momo. To obtain cDNA homologues to the Momo gene, the same library was screened again at a lower stringency with the entire cDNA fragment for Momo. Accordingly, we obtained its homologue covering the entire translation frame and named the clone Sakura. The nucleotide sequence of Sakura cDNA was 2808 bp long.

RNA analysis

PolyA + RNA was extracted and purified from adult male Sprague–Dawley rats (SLC, Shizuoka, Japan) using the acid guanidium–phenol–chloroform method (Chomczynski and Sacchi 1987). RNA samples were denatured in the presence of 50% formamide and 6% formaldehyde, separated on a 1.5% formaldehyde-agarose gel, and transferred onto a nylon membrane (Pall Scientific, East Hills, NY, USA). A ^{32}P-labeled cDNA probe was generated using the Random primed DNA labeling kit (Boehringer Mannheim). The probe (2×10^6 cpm/mL) was hybridized to filters for 20 h at 42°C in 50% formamide, 5 × sodium chloride/sodium citrate buffer (SSC), 5 × Denhardt's solution and 1% sodium dodecyl sulfate (SDS) followed by washing with 0.1 × SSC, 0.1% SDS at 60°C, and exposure to films.

In situ hybridization

Sense oligoDNAs (AGCACTGGTCCATTCAGGTTTACACCGAGTTCTGACTTTCCTACCTAC for Momo, ACAAGTCACCTCTGTGTTAGCCCAGGATCAGGAAACTCAGCAGGCCATT for Sakura) and antisense oligoDNAs (GTAGGTAGGAAAGTCAGAACTCGGTGTAAACCTGAATGGACCAGTGCT for Momo, AATGGCCTGCTGAGTTTCCTGATCCTGGGCTAACACAGAGGTGACTTGT for Sakura) were selected not to have any significant homology to other genes and labeled with terminal deoxynucleotide transferase (Toyobo Biotech, Osaka, Japan) and [α-^{35}S]dATP (New England Nuclear, Japan, ~3000 Ci/mmol) (Katagiri *et al.* 1993). Brain sections were incubated with the hybridization solution [50% formamide, 5 × SSC, 5 × Denhardt's solution, 1 mM EDTA, 0.1 M dithiothreitol (DTT) and 0.5 mg/mL denatured salmon sperm DNA] followed by the solution containing [^{35}S]-labeled oligoDNA (4×10^6 cpm/mL). After overnight hybridization at 42°C, sections were washed with 2 × SSC/4 mM DTT followed by 0.1 × SSC/4 mM DTT and dehydrated with ethanol. Sections were first processed in a BAS 2000 phosphoimager (Fuji Film, Tokyo, Japan) and then exposed to BioMax™ MS film (Eastman Kodak, Rochester, NY, USA).

Antibody production

Recombinant fusion proteins of the N-terminal portion of Momo (1–93 amino acids) and Sakura (1–103 amino acids) were produced in an *Escherichia coli* BL21 strain from a prokaryotic expression vector, pGEX–2T (Pharmacia, Uppsala, Sweden). Cell lysate from *E. coli* was purified with a gluthathione-conjugated affinity column (Pharmacia) and subjected to SDS–polyacrylamide gel elecrophoresis (PAGE). An induced protein band (36 kDa for Momo or 37 kDa for Sakura) was recovered and emulsified with Freund's complete adjuvants and used to immunize rabbits. Serum batches showing higher titers were subjected to antigen-affinity chromatography. The affinity column had a bed of Affi-Gel 10 (1 mL; Bio-Rad Laboratories, Hercules, CA, USA) that was coupled to synthetic peptides (1 mg; H-GAVRGQQSAFAGATGPFRFTPN-OH for Momo or H-LDGQPEEVPPPQGARMQAYSNPG-OH for Sakura), or the recombinant proteins used as the antigen. The peptide sequences were derived from their human orthologues (GenBank #AAM29180 for Momo and #AAM29181 for Sakura). As the antigen-affinity purified antibodies cross-reacted with many unidentified proteins (data not shown), the peptide affinity-purified rabbit antibodies for Momo and Sakura were used for immunoblotting.

Subcellular fractionation and immunoblotting

Cerebral cortex and medulla, cerebellar cortex and medulla, and their whole tissues of postnatal day 9 rats were dissected under a macroscope (Olympus, Tokyo, Japan) and homogenized with 10 volumes of 0.25 M sucrose/phosphate-buffered saline (PBS) with a Potter-type homogenizer. Cultured cells were similarly homogenized in 0.25 M sucrose/PBS. Unbroken cells and nuclei were removed by centrifugation at 600 × *g* for 10 min at 4°C. To obtain a crude mitochondrial fraction (P2), the supernatant was centrifuged at 5000 × *g* for 10 min at 4°C. Supernatants were further separated into a microsomal fraction (P3) and a cytoplasmic fraction (S3). Both S3 and P3 fractions were denatured and separated by SDS–PAGE using 4–20% gradient gel (NEN, Tokyo, Japan), and then transferred to a nitrocellulose membrane (Schleicher and Schuell, Dassel, Germany). The membrane was incubated with the affinity-purified anti-Momo antibody (10 μg/mL), anti-Sakura antibody (2.5 μg/mL), anti-GM130 (5 μg/mL; BD Transduction Laboratories, Lexington, KY, USA), or anti-catalase (10 μg/mL of Cathepsin C; Nordic Immunological Laboratories, Tilburg, the Netherlands). Immunoreactivity was detected with a goat anti-rabbit immunoglobulin conjugated to peroxidase (1 : 10 000) followed by a chemiluminescence reaction combined with film exposure (Western Lighting Chemiluminescence Reagent Plus; Perkin Elmer, Boston, MA, USA).

Expression vectors

Momo (1–381 amino acids) and Sakura (1–362 amino acids) cDNAs containing their entire coding regions were amplified by polymerase chain reaction (PCR) using KOD plus polymerase (Toyobo Biotech). The PCR products were inserted into the pCi vector (Promega Corp., Madison, WI, USA) carrying a myc-tag sequence at their amino-terminal end; pCi + myc-Momo and pCi + myc-Sakura. The N- and C-terminal portions of Momo and Sakura were deleted using the PCR technique and subcloned again into the pCi + myc vector; pCi + myc-ΔN-Momo and pCi + myc-ΔN-Sakura, and pCi + myc-ΔC-Momo and pCi + myc-ΔC-Sakura, respectively. The expression vector carrying FLAG-tagged Ub was also cotransfected into HEK293 cells; pcDNA3.1(+) FLAG-Ub (Shimura *et al.* 2000).

Modified Sindbis virus vector plasmid (pSinEGdsp#9) originated from pSinRep5 (Invitrogen, Carlsbad, CA, USA) as described previously (Kawamura *et al.* 2003). The pSinEGdsp#9 plasmid carried duplicated subgenomic promoters (Psg). The myc-tagged Momo and Sakura fragments were inserted into multiple cloning sites (Xba I-Mlu I) of the pSinEGdsp#9 vector to generate pSin + myc-Momo/EG and pSin + myc-Sakura/EG plasmids, respectively. Additionally the third Psg was inserted into pSinEGdsp#9 and used for the coexpression of FLAG-tagged Ub; pSin + myc-Momo/FLAG-Ub/EG and pSin + myc-Sakura/FLAG-Ub/EG. Viral genome RNA was transcribed using an Invitroscript™ Cap Kit (Invitrogen), and cotransfected with a helper mRNA (DH-26S) (Invitrogen) in BHK cells by electroporation (Gene Pulser, Bio-Rad). The titer of Sindbis virus vector was determined by monitoring EGFP-positive cells. Typically, the viral titer was greater than 10^8 infectious unit/mL.

Ubiquitination analysis in cells

Primary cortical cells were prepared from embryos of Sprague–Dawley rats (embryonic day 18) as previously described (Narisawa-Saito *et al.* 1999). The primary culture contained 5–10% glial population and were infected at a multiplicity of infection (MOI) of 1–2 for 1 h at 37°C. The cells were harvested at 22–24-h postinfection and lysed in solubilizing buffer [50 mM Tris-HCl (pH 7.5), 150 mM NaCl, 1% NP-40, and protease inhibitors (2 μg/mL aprotinin, 0.5 μg/mL leupeptin, and 1 μg/mL pepstatin A)]. Alternatively, pCi vectors carrying Momo, Sakura, and their mutants were transfected into HEK293 cells using an alternative calcium phosphate method (Chen and Okayama 1988). The cells were harvested at 42–44-h post-transfection, and lysed with the above solubilizing buffer. During infection or transfection, cells were often treated with 50 μM MG132 (Peptide Inc. Osaka, Japan) for 6 h unless otherwise noted.

Cell lysates were sonicated using a Handy Sonic (Tomy Seiko Co., Ltd, Tokyo, Japan) and centrifuged at 12 000 *g* for 20 min at 4°C. Protein concentrations of the supernatants were determined using a micro-BCA Protein Assay Reagent (Pierce, Rockford, IL, USA). Each supernatant including 200 μg of protein was incubated with anti-myc rabbit polyclonal antibody (1 μg) and Protein G Sepharose beads (10 μL; Amersham Pharmacia, Buckinghamshire, UK). The immunoprecipitates were eluted from the beads by boiling in 2 × SDS sample buffer and subjected to immunoblotting. The membranes were probed with anti-FLAG (M2), biotin-conjugated anti-FLAG (M2) antibodies (both from Sigma), or an anti-myc monoclonal antibody (9E10; ATCC, Manassas, VA, USA). After washing the membranes, the immunoreaction was detected with the secondary antibodies or streptoavidin conjugated to horseradish peroxidase. Bands were visualized using Western Lighting Chemiluminescence Reagent Plus (Perkin Elmer).

In vitro ubiquitination assay

Semi-purified myc-Momo and myc-Sakura were obtained from cultured cortical neurons infected with Sindbis viral vectors carrying Momo and Sakura, respectively. Culture lysate (200 μg protein) was subjected to immunoprecipitation with 1 μg of anti-myc rabbit IgG-linked protein G Sepharose beads. The immunoprecipitate served as a putative E3 Ub ligase in an *in vitro* ubiquitination assay with an ATP regenerating system (Suzuki *et al.* 1999). In brief, 50 μL of reaction mixture contained 10 μL protein G Sepharose bead slurries of the immunoprecipitate, 50 mM Tris-HCl (pH 7.5), 10 mM $MgCl_2$, 20 mM ATP, 0.5 mM DTT, 0.6 U/mL inorganic pyrophosphatase (Sigma), 5 μM MG132, 100 ng of purified recombinant mouse E1 (Ub activating enzyme) (Suzuki *et al.* 1999), 0.5–1 μM $(His)_6$-tagged E2 enzyme (Murata *et al.* 2001), 1 mg/mL bovine Ub (Sigma) and ^{125}I-labeled Ub (4×10^6 cpm). The mixture was incubated at 30°C for 2 h. After terminating the reaction by adding 3 × SDS sample buffer, 25 μL of the reaction mixture was separated by SDS–PAGE on a 4–20% gradient gel and visualized by autoradiography.

Producing bacterial recombinant Momo and Sakura, we also tested their E3 activity *in vitro* (Matsuda *et al.* 2001; Imai *et al.* 2003). cDNA for Momo and Sakura was subcloned to a prokaryotic expression vector, pMAL-p2 (New England BioLabs, Beverly, MA). Recombinant Momo and Sakura were produced in *E. coli* as a fusion protein of maltose binding protein, and purified with amylose resin (New England BioLabs). *In vitro* ubiquitination assay was carried out similarly in the presence of E1 and UbcH4 (E2).

Palmitoylation analysis

The HEK293 cells were metabolically labeled with [^{3}H]palmitic acid as described previously (Topinka and Bredt 1998). In brief,

40 h after transfection, cells were labeled with 1 mCi/mL [^{3}H]palmitic acid (50 Ci/mmol; New England Nuclear) for 5 h in the presence of cerulenin (2 μg/mL; Sigma) and fatty acid-free bovine serum albumin (10 μg/mL; Sigma). Proteins in the cell suspension (5%) were precipitated with a 50% v/v concentration of acetone to monitor whole [^{3}H]palmitic acid incorporation. The remaining cell suspension (95%) was homogenized in 0.25 M sucrose/PBS by passing through a 25-gauge needle. Unbroken cells and nuclei were removed by centrifugation at 600 × *g* for 10 min at 4°C. To obtain a soluble fraction (S) and a crude membrane fraction (P), the supernatant was centrifuged at 100 000 × *g* for 60 min at 4°C. The P fraction was solubilized with RIPA buffer [50 mM Tris-HCl (pH 7.5), 150 mM NaCl, 1% Triton X-100, 1% sodium deoxycholate and protease inhibitors]. Both S and P fractions (200 μg) were subjected to an immunoprecipitation reaction with 1 μg of anti-myc rabbit polyclonal antibody followed by western blotting or autoradiography. For autoradiography, an SDS–PAGE gel was treated with Amplify (Amersham Pharmacia) and exposed to Hyperfilm™ MP (Amersham Pharmacia) at −80°C.

Results

Novel primary structures of Momo and Sakura and their mRNA expression

We isolated a novel RING finger protein, Momo, and its structural homologue named Sakura from the rat cDNA library (Fig. 1a). Momo cDNA (2224 bp) contained the largest open reading frame, which encodes 381 amino acid residues (42695 Da), while Sakura cDNA (3107 bp) encoded a protein of 362 amino acid residues (40407 Da) (GenBank accession #AY157968 for rat Momo and #AY157969 for rat Sakura). The overall nucleotide homology between Momo and Sakura was 62% and their amino acid identity was 46%. The Pfam domain search program revealed that Momo and Sakura both contain two distinct zinc finger domains; consecutive two C2C2 zinc finger motifs (Klug and Schwabe 1995) and a RING finger motif (Freemont 2000). The duplicated C2C2 zinc finger motifs are located at the amino terminal region and the RING finger motif at the carboxyl terminal region. In addition, there is a putative site(s) for protein palmitoylation at most N-terminals of both Momo and Sakura. The double cysteine residues (Cys-Cys, Cys-X-Cys, or Cys-X-X-Cys) flanked by hydrophobic amino acids represent a potential palmitoylation signal (Mumby 1997). A GenBank search revealed that the Drosophila CG17019-PA gene has a 48% amino acid homology to Sakura over the entire coding region (Adams *et al.* 2000). Thus, Sakura is thought to be a mammalian orthologue for the Drosophila CG17019-PA gene, although a Drosophila mutant for the CG17019-PA gene has been not isolated. Their structural similarity to the RING finger proteins suggests that Momo and Sakura might function as an E3 Ub ligase.

To study mRNA distribution of Momo and Sakura, we performed northern blotting among brain regions and peripheral tissues examined in rats, a signal for Momo mRNA was detected at the 2.6-kb position and weakly at 5-kb position in the brain and testis (Fig. 1b). In contrast, Sakura mRNA appeared as multiple sizes of 1.6, 3.8 and 7 kb on northern blots. As we employed stringent washing conditions for blotting, these bands presumably reflected mRNA species produced from a single gene through alternative splicing or differential poly A addition. Relatively higher signals for Sakura mRNA were detected in the brain, liver, kidney, lung, and spleen. Only in the testis, the major signal for Sakura mRNA appeared as a 1.6-kb band. In contrast to the uniform distribution of Momo mRNA in the brain, Sakura mRNA was most enriched in the midbrain, including the pituitary and in the brain stem regions. *In situ* hybridization analysis revealed a more precise distribution in the brain: a stronger signal for Momo mRNA was detected in the pituitary as well as in the molecular layer of the cerebellar cortex (Fig. 1c). In contrast, Sakura mRNA was detected in the corpus callosum, brain stem, spinal cord and cerebellar white matter.

Cellular distributions of Momo and Sakura proteins

To confirm the distributions of Momo and Sakura in neurons or glial cells, protein lysates from cerebellar gray matter and white matter were prepared and subjected to western blotting (Fig. 2). When Momo and Sakura genes were overexpressed in cortical cultures containing neurons and glial cells, Momo immunoreactivity appeared as four bands around 38–45 kDa, and the Sakura immunoreactivity as two bands around 46 kDa and 40 kDa (Fig. 2a,b; left). Some bands exhibited higher or lower mobility in a gel in comparison with their calculated molecular sizes. The mobility shift might reflect their post-translational modifications including palmitoylation, myristylation, and proteolytic processing (Kahns *et al.* 2002). Momo immunoreactivity was most enriched in the gray matter fractions of the cerebral cortex and cerebellar cortex while Sakura immunoreactivity was recovered mainly in the white matter fractions. The sizes of the endogenous Momo and Sakura immunoreactivities matched those in positive controls. Momo and Sakura lack a transmembrane region and a typical signal peptide motif for membrane anchoring, but they both carry putative palmitoylation site(s) in the N-terminal region to interact with the membrane via a fatty acid moiety (Resh 1999). The membrane (P3) and cytoplasmic (S3) fractions were prepared from the cerebellum. Western blotting of each fraction revealed that the immunoreactivity for both Momo and Sakura was enriched in the membrane fraction. Almost none of the Sakura immunoreactivity was recovered in the cytosolic fraction.

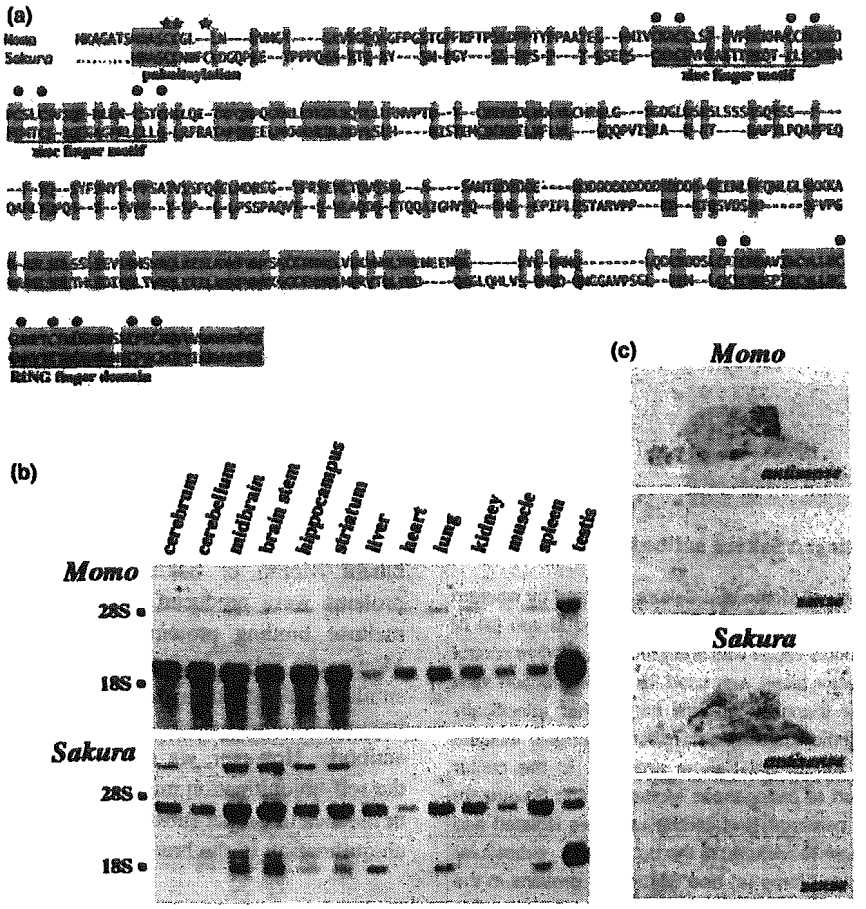

Fig. 1 Structure and tissue distributions of Momo and Sakura. (a) Deduced amino acid sequence is aligned for Momo and Sakura. Identical amino acids are boxed in gray. Gaps between conserved amino acids are indicated by dashes. Core residues of C2C2 zinc finger and RING finger are marked with closed circles. Asterisks indicate putative palmitoylation sites. (b) Northern blot hybridization was performed with the poly(A) + mRNAs extracted from six areas of the brain as well as seven tissues from peripheral organs. The membrane was hybridized with the random [^{32}P]dCTP labeled 370-nt *Dra* I-*Dra* I *Momo* cDNA fragment or the 292-nt *Stu* I-*Stu* I *Sakura* cDNA fragment. (c) *In situ* hybridization was performed with sagittal sections (10-μm thick) of adult rat brain. Each section was probed with the sense or antisense oligoDNAs, which were end-labeled with [^{35}S]dATP. Sense and antisense probes for *Momo* contained 48 base oligoDNA (nt. 103–150) in the ORF (upper panel). Sense and antisense probes for *Sakura* contained 49 base oligoDNA (nt. 546–594) in its ORF region (lower panel).

Ubiquitination induced by overexpression of Momo and Sakura in cortical culture

Using rat cortical cultures containing both neurons and glial cells, we assessed their biological activity as a Ub ligase. Myc-tagged Momo and/or FLAG-tagged Ub were overexpressed in cultured cortical cells using the Sindbis virus expression system (Kawamura *et al.* 2003) (Fig. 3a). Incorporation of FLAG-tagged Ub into total protein was monitored by western blotting using the anti-FLAG antibody (Fig. 3b). When cortical cultures were transfected with the viral vector carrying FLAG-tagged Ub alone, basal ligation of the tagged-Ub was only detected in the presence of a proteasome inhibitor, MG132, as observed by broad bands. There was no apparent influence of the Momo expression on total ubiquitination levels. We also examined Momo-dependent ubiquitination in the immune complex of an anti-myc antibody (Fig. 3c). The overexpression of myc-tagged Momo induced polyubiquitination of target protein(s) in the Momo-carrying immune complex. The ubiquitination was less pronounced in the absence of the proteasome inhibitor, MG132. Although cortical neurons endogenously expressed Momo, basal reaction of ubiqutination was almost undetectable because the strength of basal Momo expression was less than one hundredth of that by Sindbis virus-mediated overexpression (data not shown). Thus, these results suggest that Momo is involved in polyubiquitination.

When myc-tagged Sakura was similarly expressed by a Sindbis virus expression vector together with FLAG-tagged

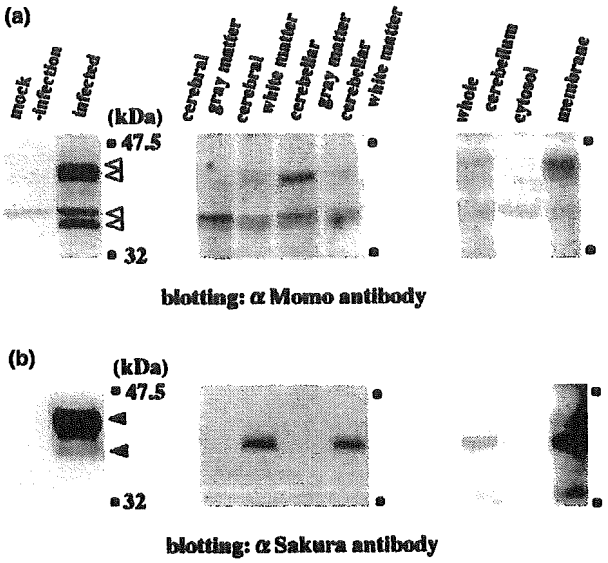

Fig. 2 Cellular distribution of Momo and Sakura detected by western blot using their autologous antibodies. Overexpressed Momo (a) or Sakura (b) protein by Sindbis vector was analyzed as a positive control (left panels). Sindbis vector alone was used for mock infection as a negative control. Open triangles indicate bands that specifically reacted with an anti-Momo antibody and closed triangles indicate immunoreactive bands for an anti-Sakura antibody. In the center panels, tissue distribution of endogenous Momo (a) and Sakura (b) proteins is shown. The cerebrum and cerebellum were isolated and separated into gray and white matters. In the right panels, subcellular localization of endogenous Momo (a) and Sakura (b) proteins in the cerebellum. Cytoplasmic fraction (S3) and microsomal fraction (P3) were indicated as cytosol and membrane, respectively.

Ub, a similar ubiquitination reaction in the absence of the MG132 was observed in total ubiquitination as well as in the immune complex of Sakura (Fig. 4). In contrast to the reaction with Momo, however, marked amounts of poly-ubiquitinated protein(s) induced by the Sakura expression were not influenced by the presence or absence of the inhibitor, MG132. The results suggest that the ubiquitination by Sakura is relatively stable and might not be recognized by the conventional MG132-sensitive 26S proteasome (Hershko and Ciechanover 1998).

In vitro ubiquitination of Momo and Sakura and their interaction with various E2 components

We attempted to reconstitute the ubiquitination *in vitro* with a purified recombinant Ub activating enzyme (E1) and various Ub conjugating enzymes (E2; Ubc) as well as Momo or Sakura as a Ub ligase (E3). Each UbcH3, H4, H5c, H6, and H8 was tested as an E2 enzyme and ubiquitination reaction was monitored *in vitro* in the presence of ^{125}I-labeled Ub. The combination of immunoprecipitated myc-tagged Momo with UbcH4 and H5c, but not with UbcH3, H6, nor H8, triggered ubiquitination (Fig. 5a). The immune complex of myc-tagged Momo alone failed to induce ubiquitination (data not shown). Western blotting for the anti-myc antibody suggested that the polyubiquitination might include self-ubiquitination of Momo as the amounts of authentic Momo were reduced and its size shifted to higher molecular ranges, although the shift was not apparent in the ubiquitination assay using cultured neural cells (see Fig. 3c). In contrast, myc-tagged Sakura recruited UbcH4, H5c and H6 to induce polyubiquitination (Fig. 5c). In contrast to the potential self-ubiquitination of Momo, the Sakura-induced self-ubiquitination was not apparent in the western blots with the anti-myc antibody. In the absence of Momo or Sakura, however, there was no endogenous ubiquitination (Fig. 5b).

To avoid the possibility that the immune complexes carried not only Momo or Sakura but also other E3 enzyme(s) and thus caused the *in vitro* ubiqutination, we attempted to reconstitute the reaction using purified recombinant Momo or Sakura (Fig. 5d). Momo and Sakura proteins were produced in *E. coli* as a fusion protein of maltose binding protein. Incubation of the recombinant Momo and Sakura with the purified E1 enzyme and UbcH4 similarly caused their self-ubiquitination as monitored by immunoblotting using the anti-maltose binding protein antibody. However, we cannot rule out the possibility that the self-ubiquitination might result from their overexpression or the lack of proper substrates, as we failed to detect the self-ubiquitination in the brain or neural cells.

Dependency of ubiquitination on C-terminal RING finger

The structural dependency of Momo- and Sakura-mediated ubiquitination was examined in a human embryonic kidney cell line, HEK293. We produced deletion mutants of myc-tagged Momo and Sakura, omitting their N-terminal portion containing the palmitoylation sites/double zinc finger domain (ΔN) or their C-terminal region containing the RING finger domain (ΔC) (Fig. 6a). The transfection of cDNA for wild-type Momo and Sakura as well as that for mutants resulted in a significant level of protein expression in HEK293 cells, although the N-terminal deletion appeared to reduce their stability (Fig. 6b). The transfection of wild-type Momo cDNA together with the FLAG-tagged Ub increased Ub immunoreactivity as revealed with the anti-FLAG antibody (Fig. 6c). The deletions in the N-terminal as well as in the C-terminal of Momo significantly diminished the Ub immunoreactivity in the ubiquitination reaction in culture. In contrast, while the C-terminal deletion mutant of Sakura almost completely abolished the ubiquitination reaction, its N-terminal deletion only influenced the sensitivity of the Sakura-induced ubiquitination to the proteasome inhibitor, MG132, but not the ubiquitination itself (Fig. 6d). These results confirm that the RING finger domain of Momo and Sakura has a primary role in ubiquitination.

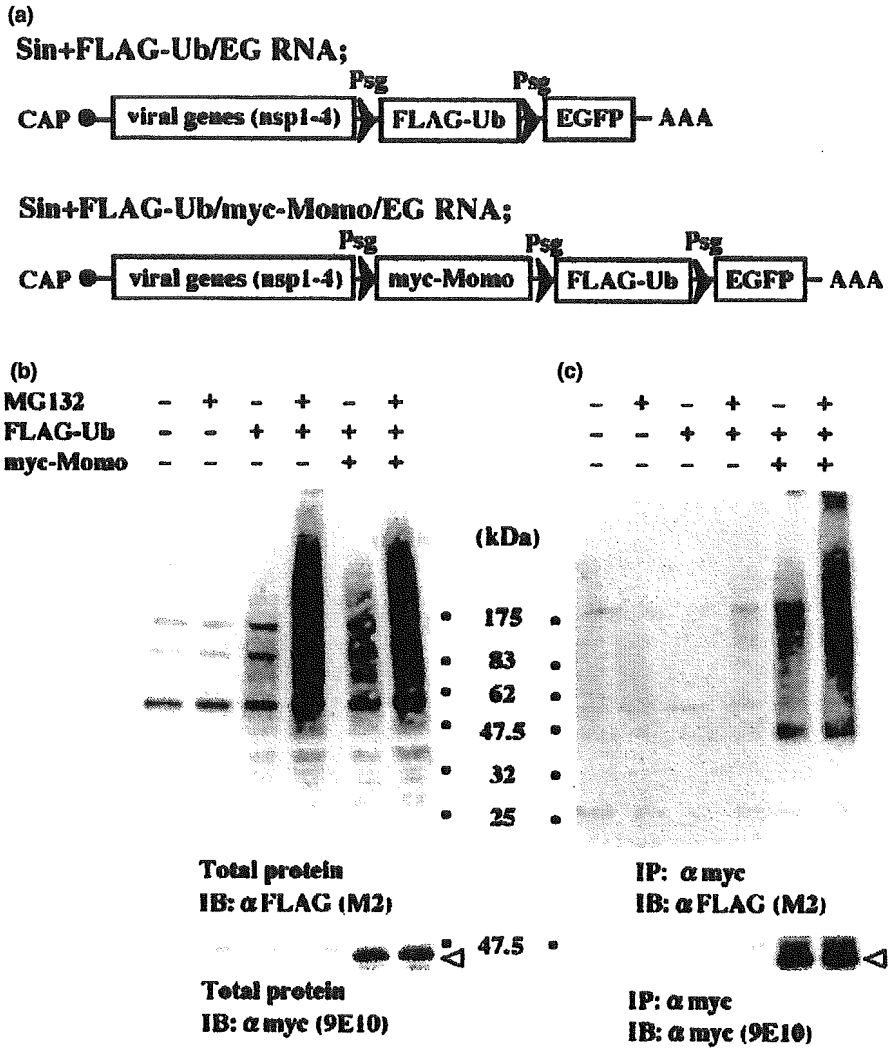

Fig. 3 Ubiquitination assay of Momo protein in cortical culture. (a) Structures of recombinant Sindbis virus RNA: the upper is a FLAG-Ub expression construct and the lower is a coexpression construct for myc-Momo and FLAG-Ub. The duplicated/triplicated subgenomic promoter (Psg), viral replication essential genes (nsp1–4), cap-dependent translation initiation site (CAP), and polyA tail (AAA) are indicated. Virus infectious units were determined by the expression of the enhanced green fluorescent protein (EGFP) and adjusted among cultures. (b) Overexpression of myc-Momo and/or FLAG-Ub proteins in cortical culture. Total cell lysates were subjected to western blotting using the anti-FLAG (M2) antibody (top) and anti-myc (9E10) antibody (bottom). (c) Ubiquitinated protein(s) in the immunocomplexes with myc-Momo. Immunoprecipitated protein complexes prepared by an anti-myc polyclonal antibody were subjected to immunoreaction with the anti-FLAG antibody for ubiquitination (top) and anti-myc antibody (9E10) for Momo (bottom). There was no apparent mobility shift of myc-Momo (data not shown). Open triangles indicate Momo immunoreactivity.

Membrane association via the N-terminal domain of Momo and Sakura

Using the above deletion constructs, we also monitored subcellular localization of the Momo and Sakura mutant proteins. Wild-type Momo and Sakura as well as the mutant proteins were overexpressed in HEK293 cells, and subsequently the cells were fractionated into crude membrane and cytoplasmic fraction (Fig. 7a). Subcellular fractionation was confirmed by immunoblotting for a Golgi-associated protein, GM130, and a cytoplasmic enzyme, catalase. The cytoplasmic fraction contained larger amounts of catalase while the membrane fraction carried predominantly higher levels of GM130 in all preparations. Synthesized wild-type myc-tagged Momo and Sakura had similar molecular sizes to those in neural culture (see Fig. 2a,b) and were recovered in both the membrane and cytoplasmic fractions under the fractionation condition. In contrast, when cells expressing the Momo and Sakura mutants lacking the N-terminal domain